

Context-conditioned generative models enable sub-national refinement of sparse humanitarian survey data

Federica Sibilla¹, Vasiliki Voukelatou^{2*}, Duccio Piovani²,
Kyriacos Koupparis², Daniela Paolotti¹, Rossano Schifanella^{3,1},
Kyriaki Kalimeri^{1,4*}

¹ISI Foundation, Torino & 10123, Italy. ²World Food Programme, Rome & 00148, Italy.

³Computer Science, Università di Torino, Turin & 10124, Italy. ⁴UNICEF, New York & 10038, USA.

*Corresponding author. Email: vasiliki.voukelatou@wfp.com, kyriaki.kalimeri@isi.it

Data scarcity limits inference in many scientific and policy domains. Survey data are essential for decision-making, but sparse samples often fail to capture fine spatial granularities. We evaluate normalizing flows, a generative AI model that learns complex data distributions and can be conditioned on exogenous contextual features, in controlled data scarcity scenarios. Across eight household survey datasets spanning six low-income or middle-income countries in the humanitarian domain, we show that context-conditional generative models improve sub-national distributional estimates beyond oversampling, while conditioning on region labels alone yields limited gains. These findings support a general principle for survey data augmentation: generative models can improve sub-national estimates when the sparse sample retains sufficient support and contextual covariates encode relevant local heterogeneity. By learning full household-level conditional distributions rather than aggregate point estimates, the approach is well suited to small-area es-

timation and can better characterize local heterogeneity in humanitarian settings requiring fine-grained evidence for targeting and resource allocation.

Introduction

Many scientific and policy domains rely on data that are sparse, costly to collect, or unevenly distributed across space and populations. Yet decision-making often requires fine-grained estimates of distributions and aggregates at sub-national levels and across demographic groups (1, 2). Classical small-area estimation approaches address this gap by borrowing strength across areas to estimate aggregate indicators such as means, totals, or poverty rates (3, 4), but they do not reconstruct the full household-level distributions from which multiple indicators can subsequently be derived. This tension is especially acute in humanitarian settings, where household surveys are the primary instrument for informing operational decisions. Food security assessments such as World Food Programme’s (WFP) Vulnerability Analysis and Mapping surveys guide targeting and resource allocation for hunger response (5); socioeconomic surveys such as the World Bank Living Standards Measurement Studies inform poverty mapping and social protection design (1); and child welfare surveys such as UNICEF’s Multiple Indicator Cluster Surveys (MICS) provide the evidence base for national policy on education, nutrition, and child protection across more than 120 countries (6). Yet data collection in these settings remains expensive, infrequent, and difficult to implement in vulnerable or unstable environments, particularly in conflict-affected areas. In these contexts, researchers and practitioners often need to draw detailed inferences from samples that are too limited to recover local heterogeneity reliably.

Recent advances in generative artificial intelligence have enabled the synthesis of realistic tabular data and the modeling of complex conditional distributions (7–13). This has motivated researchers to apply generative models for survey data generation. Applications have largely focused on synthetic population generation for downstream agent-based model simulations, spatial microsimulation, and privacy-preserving data release (14–18). More recently, generative models have been explored as an augmentation tool in the health domain, to enlarge the training set of downstream machine learning models when clinical data are scarce (19). This latter role in statistical inference under data scarcity remains much less established (20). A fundamental challenge is that generative models cannot

create information absent from the training sample: when the training data are non-representative, biased or incomplete, the model will reproduce and may even amplify these limitations rather than correct them (21–23).

Building on the above, previous work has mostly focused on improving the fidelity of synthetic data while preserving privacy, giving less attention to the conditions under which generative models can meaningfully contribute to inference. Crucially, many of the target outcomes measured by household surveys are structurally related to contextual characteristics of a place, including market accessibility, relative wealth, and environmental conditions (24–27). These contextual signals are increasingly available at fine spatial resolution from satellite imagery, mobile phone networks, and remote sensing products, independently of survey collection (28, 29). This motivates a fundamental question: under what conditions can generative models integrate exogenous contextual information with sparse survey data to serve as genuine inference tools? This question is critical because many applications require more than plausible synthetic records. They require reliable estimates of local distributions and aggregate indicators in settings where direct measurement is limited.

In this work, we address this question in the context of humanitarian household survey data, where sparsity, heterogeneity, and sampling constraints are pervasive. We introduce a conceptual and empirical framework based on conditional generation (Figure 1): a normalizing flow (30) (cNF), a generative AI model, is trained on a sparse, yet nationally representative household survey subsample and conditioned on contextual features, including market accessibility (28), relative wealth indices (26), and environmental indicators (29), which are available at fine spatial resolution independently of any data collection. Assuming these relationships are spatially homogeneous within a country, the model that learns how place-level signals modulate the distribution of household-level outcomes can generate synthetic household records for under-sampled (or even unsampled) locations by conditioning on their known covariate values, thereby refining local distributional structure that is only weakly represented in the sparse sample. We simulate controlled data scarcity by subsampling household survey data to deliberately disrupt sub-national representativeness while preserving national-level composition. This methodological framework is applied across eight nationally representative surveys spanning six low-income or middle-income countries - Ethiopia, Sri Lanka, Mozambique, Nigeria, Zimbabwe and Yemen were selected as priority humanitarian contexts, and comparable survey data availability enabling consistent contextual feature construction

(table S1). We then evaluate whether the generated data better approximate sub-national distributions and aggregate indicators than an oversampling baseline of the observed sample. We test whether generative refinement improves estimates by comparing the context-conditioned model (cNF) with two versions of the normalizing flow: a model conditioned solely on a categorical geographical-region label (NF), and a model conditioned on both the geographical-region label and sector, with sector representing the rural/urban classification (NF + sector). This comparison helps isolate continuous contextual features as the source of additional generative improvement. Standard tabular generative models, including CTGAN and TVAE (9), are not included in the main inferential analysis because they do not provide a natural mechanism for explicitly conditioning generation on continuous external covariates at both training and generation time, which we require to generate records for under-sampled or unsampled locations. Instead, we include them in a separate supplementary benchmark (23), training on the full survey data, to evaluate general synthetic-data quality in terms of fidelity and originality against the full population (31). Across datasets, cNF achieves fidelity–originality trade-offs comparable to or better than these widely used tabular generative models (figure S4), indicating that the observed inferential gains are not attributable to an unusually weak generative baseline.

Our results show that context-conditioned normalizing flows applied to scarce survey data—where context is represented as exogenous features linked to environmental, wealth, accessibility indicators, and settlement type—provide more accurate, higher-resolution estimates than simple baseline models. We also explore the utility of generated data for small-area estimation, and show that it depends on the intrinsic variability of the target distribution: the value of refinement increases when sub-national distributions differ strongly from the national distribution, and declines as sample size increases.

Taken together, these findings support a general principle: generative models can become powerful inference tools when paired with informative external features. By formalizing and testing this principle across diverse survey settings, our work contributes both a conceptual and a practical framework for using generative models as complements to scarce survey data. Importantly, it provides practitioners with empirical guidance on when deploying this framework is likely to add value, particularly in humanitarian contexts where fine-grained evidence is needed but difficult to collect.

Results

Context-conditional generative AI enables sub-national refinement

We compared three conditioning strategies under severe scarcity (one PSU per ADM1 region): full geospatial context (cNF), region plus sector (NF+sector), and region only (NF). Conditioning on a categorical region label (NF) yields only marginal improvement over oversampling, adding sector (NF+sector) yields further gains, and conditioning on the full set of contextual features (cNF) yields systematic performance gains across datasets and generated target variables. Figure 2 quantifies improvement over the oversampling baseline under two complementary metrics: panel A reports improvement in Earth Mover’s Distance (EMD), which measures distributional fidelity at the sub-national level, and panel B reports improvement in Mean Absolute Error (MAE), which measures the accuracy of sub-national mean estimates. Both panels display the same three conditioning strategies (cNF, NF+sector, NF). Because all three variants share the same flow architecture, the monotonic improvement from NF to NF+sector to cNF indicates that performance gains are driven by the informational content of the conditioning variables. Unlike Figure 2, where improvements are measured relative to oversampling, the following Shapley analysis isolates the contribution of continuous contextual information by defining improvement relative to the NF+sector model, thereby removing the effect of sector conditioning and attributing performance gains specifically to additional contextual covariates. We examine the contribution of each contextual feature group to the improvement achieved by the cNF model, quantified using Shapley values. The three groups are relative wealth (W), market accessibility (M), and environment (E). This attribution is quantified via a Shapley value decomposition defined on performance gains rather than on model outputs, distinguishing it from standard SHAP-based interpretability methods. Figure 3 shows that most contextual feature groups contribute positively on average, but contributions vary across datasets and target domains, indicating that no single contextual signal is universally informative. In Ethiopia, wealth- and market-accessibility-related conditions contribute positively and consistently, whereas the contribution of environmental conditions is more mixed. In Nigeria MICS dataset, wealth and market accessibility show a higher contribution, compared to environmental context which shows a less stable contribution. These results suggest that no single covariate dominates globally. Instead, the performance gains of the fully context-informed cNF model reflect the cumulative

and dataset-specific signal carried by multiple exogenous contextual features beyond the sector-level conditioning already available to the model. A supplementary analysis suggests that ADM1-level predictability of target means from contextual features is moderately associated with lower cNF aggregate error (Pearson= -0.47 , Spearman= -0.49 ; negative correlations indicate that higher ADM1-level predictability is associated with lower cNF error), but this metric does not fully explain generative gains, which depend on distributional rather than only mean-level structure ((23), Supplementary Text, figure S1, figure S2).

Sensitivity to training sample size

To assess how training sample size affects the performance gains of the cNF model, we repeated the experiments varying the size of the nationally representative subsample. Here, a primary sampling unit (PSU) denotes the survey cluster used as the unit of subsampling; all datasets were subsampled at the PSU level, with the exception of the Yemen mVAM dataset, where households were sampled directly. Consequently, Yemen results should be interpreted as illustrating the same scarcity principle under a different sampling design rather than as directly comparable on the x -axis of Figure 4. Across all datasets, when the subsample is minimal—comprising one PSU per sub-national region, performance improvements are largest and most heterogeneous, reflecting the acute information gap that contextual features help fill (Figure 4). As the number of PSUs increases, the magnitude of the baseline error itself declines monotonically toward zero, as the subsample becomes increasingly representative of the underlying population. Intuitively, this convergence indicates that the marginal value of contextual features diminishes as direct survey information becomes more abundant.

Improvements are widespread but heterogeneous

Figure 5 maps the regional difference in EMD between the oversampling baseline and cNF (baseline – cNF) for each dataset and target variable. Across most datasets and targets, improvements are spatially widespread, indicating that cNF generally enhances distributional representativeness relative to the oversampling approach. Variable-level significance, assessed with one-sided paired t -tests across regions and seeds with BH-FDR correction, confirms that improvements are significant

for nearly all dataset–target combinations, with Ethiopia ESS vitamin B12 as the only non-significant case; this exception is consistent with the very low and nearly spatially invariant vitamin B12 values across the country, which leave little sub-national variation for either the baseline or cNF to capture. At the same time, the maps reveal substantial heterogeneity in these gains, with some regions and variables showing modest gains or occasional reversals where cNF underperforms the baseline. This spatial variation suggests that the benefits of deploying context-conditioned generative AI are not uniform: the same model can substantially improve estimates in some regions while offering limited advantage in others. When considering where the overall difference between cNF and the baseline is significant, we see that, with only one exception in Nigeria for the NLSS dataset, the differences are in favor of cNF.

Competitive aggregate estimates with distributional outputs

Having established that cNF consistently outperforms oversampling in distributional fidelity, we next examine its performance on aggregate statistics. We compare cNF to a Bayesian multivariate linear regression model fitted on the same set of contextual features. For each observation, the Bayesian model yields a Gaussian posterior predictive distribution characterised by a mean and standard deviation; regional estimates are obtained by aggregating these summaries across observations within each administrative unit. Because the Bayesian baseline produces Gaussian predictions rather than household-level synthetic records, the comparison is restricted to aggregate MAE, the quantity for which both methods provide directly comparable outputs (Figure 6A). The cNF model achieves modest but statistically significant improvements over the Bayesian regression baseline (paired one-sided Wilcoxon signed-rank test, $p = 0.003$). This indicates that context-conditional generation is a competitive complement to statistical methods typically employed for aggregate value inference under data scarcity. Crucially, cNF additionally produces individual household-level records conditional on local contextual features, making it possible to inspect estimated local distributional shapes, compare tails and modes, and perform distributional diagnostics that are not available from aggregate Gaussian predictions. We therefore interpret panel C in Figure 6 as an illustration of the additional information made available by the generative framework. This is particularly useful when small-area descriptions are needed that go beyond aggregate values, for

example, by examining the characteristics of households at risk of food insecurity, including the settings where machine learning models are already used to predict outcomes such as the risk of micronutrient inadequacy (27).

Refinement is most useful when regional variability is high

We assess whether the refinement gains achieved by cNF are sufficient to produce sub-national distributions that are more representative than simply assigning the nationally representative distribution from the subsample to each sub-national region. Figure 7 compares three quantities: intrinsic sub-national variability, defined as the EMD between the true (full) national and true (full) sub-national distribution (blue), EMD between true distribution and national subsample used for training (orange), and EMD between true distribution and cNF-generated data (green). Regions are ordered by intrinsic sub-national variability. When intrinsic sub-national variability is low, the national subsample provides a reasonable approximation, and cNF offers no additional benefit. As variability increases, cNF more frequently achieves lower EMD than the national baseline, with the magnitude of improvement growing with variability. This result indicates that generative refinement is most useful in settings where local distributions differ substantially from the national average. However, intrinsic variability as defined here requires knowledge of the true national and sub-national distributions, which is precisely the information unavailable to a practitioner deciding whether to deploy cNF.

To assess whether this circularity can be partially resolved, a supplementary analysis trains a classifier to predict, from *sample-based* proxies alone — intrinsic variability estimated from the sparse subsample and sample size — whether cNF refinement yields a positive improvement relative to the national baseline (23). The classifier achieves a ROC AUC of 0.63 on the held-out test set. This suggests limited predictive signal: sample size and intrinsic variability contain some information about when cNF refinement is likely to help, but they do not close the decision loop. Dataset-specific factors that are not reducible to these two quantities still play an important role, and the classifier should not be treated as an operational decision tool.

Taken together, these results delineate the conditions under which conditional generative refinement is most beneficial for high-resolution sub-national estimation: gains are largest when

contextual features are informative, when training samples are small, and when local distributions diverge substantially from the national average — precisely the constellation of conditions that characterize data-scarce humanitarian settings.

Discussion

Our results support a simple but consequential principle that follows directly from how generative models work: while they cannot create missing information *de novo*, they can serve as inference tools when informative contextual features enable the recovery of local structure that is poorly represented in the sample. When contextual features encode a signal about sub-national heterogeneity, a conditional normalizing flow can redistribute that signal across the spatial domain, producing synthetic distributions that are more locally representative than those obtained through mere resampling of the observed data alone. Without informative contextual features, the generative model does not yield consistent improvements and largely reproduces the behavior of simple resampling. This result reflects a generative instantiation of a classical problem in statistical inference: when the covariate distribution at training time differs from the covariate distribution at prediction time — a setting formalised as covariate shift (32) — standard estimators degrade, and recovery requires leveraging the relationship between features and outcomes to reweight or redistribute information across the target domain. Here, rather than reweighting, the model learns this relationship explicitly and uses it to generate plausible outcomes at poorly represented covariate values. Our framing contributes to the debate on whether generative augmentation of tabular data can ever be of any practical use for inference tasks (20). The key issue may be less about whether the architecture is sufficiently expressive and more about how to incorporate additional information to support improved inference.

Because all three conditioning variants share the same flow architecture, the monotonic gains from NF to NF+sector to cNF isolate the conditioning signal as the driver: coarse categorical labels allow only group-average distributions, whereas continuous contextual features carry fine-grained spatial information that enables the model to generate plausible outcomes for poorly represented locations. This is the mechanism by which generative models incorporate information: they redistribute structure within the support of the covariate space, rather than extrapolating beyond

the support of the outcome space.

Practical implications. In practice, the framework is most useful when: (i) informative contextual covariates are available, (ii) survey samples are sparse at the target spatial resolution, and (iii) local distributions differ from national averages. When these conditions are absent, simpler approaches such as oversampling or direct resampling may be sufficient.

Our objective differs from classical small-area estimation approaches such as Fay–Herriot (3) or unit-level models (4), which are primarily designed to estimate aggregate indicators such as means, totals, or prevalence rates. In contrast, the proposed framework aims to reconstruct full household-level distributions from which multiple indicators can subsequently be derived. For this reason, we compare aggregate performance against a Bayesian regression baseline while evaluating distributional performance separately through EMD-based metrics. Future work could explore integration with established small-area estimation frameworks.

While context-conditional generative models consistently improve sub-national distributional estimates over simple oversampling, the quality of the training sample remains a foundational prerequisite. Because both cNF and oversampling inherit the support of the training sample, relative improvement over oversampling should not be interpreted as correction of sampling bias. Our framework assumes national-level representativeness with respect to the dimensions relevant to the target variable; generative refinement leverages the information present in the sample but does not correct for its structural deficiencies. A supplementary analysis examines urban-biased sampling, where rural households are systematically excluded (Supplementary text, figure S3). Contextual conditioning can still improve relative to oversampling within the same biased regime, but absolute error for socioeconomic outcomes increases when rural households are excluded.

Several limitations of the current analysis deserve acknowledgment. Our framework assumes that relationships between contextual variables and survey outcomes are sufficiently stable across space. Performance may degrade when these relationships vary systematically across regions. The most consequential manifestation of this assumption is that the covariate–target relationship, $p(Y | X)$, is treated as stationary across space. The model learns a single conditional distribution from the pooled national sample and applies it to all regions; if regional ecology, market integration, cultural factors, or conflict exposure give rise to localized relationships that differ from the national average,

the generated distributions may be systematically biased in those regions. The present evaluation does not directly test this assumption: in the severe scarcity setting every ADM1 contributes at least one PSU to the training sample, so the model always observes some data from each region. A stronger test would be a leave-region-out validation in which one or more ADM1s are entirely excluded from training and generation quality is evaluated on those held-out regions. If cNF still improves over the national baseline in this setting, it would provide more direct evidence that the learned conditional transfers across space; if it does not, it would delineate the spatial scope within which the stationarity assumption is defensible. We consider this an important direction for future work.

A second structural limitation is that the current framework is restricted to continuous target variables because training the cNF model requires continuous outcomes. Extending this approach to include mixed-type variables is beyond the scope of this work, but would broaden its practical applicability.

Furthermore, the contextual features used for conditioning are themselves model-derived products, often constructed from remote sensing and mobile connectivity data, and may contain substantial measurement error not explicitly accounted for in our framework. The Shapley analysis confirms that contextual variables occasionally show negative contributions for specific dataset–target combinations, indicating that external context can introduce noise rather than useful signal. Future work could extend the conditioning set with additional humanitarian covariates such as conflict exposure, displacement patterns, and market disruptions. A related limitation is that household geolocation data are typically coarsened to protect privacy, so conditioning information remains spatially aggregated and cannot fully capture micro-level heterogeneity. Conversely, generating household-level records conditional on fine-grained location features could raise re-identification risk; any operational deployment should assess disclosure risk relative to the spatial resolution and population density of the target domain.

A further limitation arises from the evaluation of model performance. Although the model is trained on the joint distribution of all variables, the metrics are computed separately for each variable. As a result, errors in the dependence between variables are not captured, even though such relationships may be important for joint outcomes.

Finally, the empirical scope of this study is limited to humanitarian household surveys. Al-

though the datasets span multiple countries and outcome domains, they share broadly similar survey structures. The same logic may be relevant to other settings where outcomes are spatially structured and direct measurement is sparse — including epidemiological surveillance, poverty mapping, and agricultural yield estimation — but generalization will require dedicated empirical validation. Looking forward, a promising development is the emergence of foundation models that encode multi-modal descriptions of place into task-agnostic spatial embeddings that can serve as conditioning inputs for downstream models (33).

Taken together, our results show that context-conditioned generative models can extract additional inferential signal from sparse survey data when external contextual features are informative about local variation. Household surveys offer a paradigmatic case: direct measurement is costly, spatial coverage is often uneven, and decisions frequently require estimates below the level at which samples are fully representative. At the same time, our findings also clarify the limits of this approach. Generative refinement is most useful when the available sample is insufficiently representative at the target spatial resolution, when local distributions differ meaningfully from the national distribution, and when contextual features capture part of that local variation. When these conditions are not met, simpler baselines may perform similarly. The framework developed here, therefore, provides a practical basis for assessing when contextual information can yield reliable inferential gains and when generative augmentation is unlikely to justify its added complexity.

Materials and Methods

Problem formulation

We study the problem of estimating sub-national distributions and aggregate statistics from sparse household survey data. Let $Y \in \mathbb{R}^d$ denote a vector of continuous target variables of interest (e.g., food security or socioeconomic indicators). Let $\ell \in \{0, 1, \dots, L\}$ denote a level of administrative resolution, where $\ell = 0$ corresponds to national level, $\ell = 1$ to first-level administrative resolution and $\ell = L$ to the finest available level. At each level, let $a_\ell \in \mathcal{A}_\ell$ denote the sub-national region

index of a given household¹, where \mathcal{A}_ℓ is the set of regions at level ℓ . Let $s \in S$ denote the sector a given household belongs to (rural, urban, estate)², and let $X \in \mathbb{R}^p$ denote a vector of contextual features (e.g., accessibility, wealth proxies, environmental indicators).

Our inferential target is the regional distribution $p(Y | a_1)$: the distribution of household-level outcomes within each first-level administrative unit, aggregated over sector. During model training, sector membership and contextual covariates are incorporated as conditioning information, so that the generative model learns distributions of the form $p(Y | a, s, X)$. Regional distributions are then obtained by aggregating over the known sector composition:

$$p(Y | a) = \sum_s p(Y | a, s, X_a) p(s | a), \quad (1)$$

where $p(s | a)$ is treated as known from the survey design. Sector is therefore not part of the target but part of the conditioning structure used to improve estimation; its regional composition is typically available from survey metadata or census data. All evaluations are performed at the ADM1 level by comparing generated and observed regional distributions $p(Y | a_1)$.

Consider a limited sample of household observations $\{(Y_i, a_{L,i}, s_i)\}_{i=1}^n$ that is representative only at national level $\ell = 0$ with respect to spatial and sector dimensions, and can therefore only be used to estimate $p(Y | a_0)$. By enriching this sample with contextual features, so that it becomes $\{(Y_i, X_{a_{L,i}}, s_i)\}_{i=1}^n$, and assuming that the relationship between X and Y is homogeneous across space, we train a generative model to learn $p(Y | X, s)$. This learned conditional can then generate synthetic household-level data for any region a_ℓ for which contextual features are available, by sampling $Y_i \sim p(Y | X_{a_\ell}, s)$.

Data scarcity simulation

We treat each full survey dataset $D = \{(Y_i, a_{L,i}, s_i)\}_{i=1}^m$, representative at the sub-national level by design through two-stage cluster sampling (34), as ground truth. From D we construct a sparse training sample D' by subsampling at the primary sampling unit (PSU) level, since PSUs are the operational units through which household surveys are implemented in the field. PSU selection is

¹For privacy protection, household locations are typically available only at an aggregated spatial resolution, usually up to the first- or second-level administrative unit

²Estate sector is present only in Sri Lanka

stratified within each first-level administrative unit so that the rural–urban composition of D' approximates that of D ; the resulting subsample therefore preserves national-level spatial and sectoral composition while, by construction, destroying sub-national representativeness. In the most severe scarcity setting, one PSU is selected per first-level administrative unit (typically ~ 10 households per PSU, with variation across clusters). The Yemen mobile VAM dataset is an exception: since mobile surveys do not rely on PSUs, households are sampled directly.

We denote by $\tilde{D} = \{(Y_i, X_{a_{L,i}}, s_i)\}_{i=1}^{m-n}$ the held-out observations excluded from D' . Contextual features are attached to all households at the finest available administrative resolution, so that D' becomes $\{(Y_i, X_{a_{L,i}}, s_i)\}_{i=1}^n$. A conditional normalizing flow is trained on the enriched D' and used to generate target values for the held-out locations: $Y_j^{\text{gen}} \sim p(Y|X_{a_\ell}, s)$. The generated set $G = \{(Y_i^{\text{gen}}, X_{a_{L,i}}, s_i)\}_{i=1}^{m-n}$ is evaluated against \tilde{D} by comparing distributions and aggregate means at the first-level administrative resolution. All subsampling steps are repeated with five independent random seeds; results in figures 2–7 are averaged across seeds. Figure 1 offers a visual representation of the framework.

Sample size sensitivity

To characterise robustness under varying degrees of data scarcity, we repeat all experiments while varying the number of PSUs selected per first-level administrative resolution region from 1 (extreme scarcity) to 8 (moderate scarcity). All methods are evaluated under identical sampling conditions for each setting. For each level of data scarcity (PSU count), we compute performance improvements across many scenarios (regions, variables, seeds), and then summarise them into a single average trend. To capture variability in performance, we also report one standard deviation across regions and variables. These results are summarised in Figure 4.

Datasets

We evaluate our approach on eight household survey datasets spanning diverse geographic and socioeconomic contexts (Table S1). All surveys use a two-stage stratified cluster sampling design in which households are nested within primary sampling units (PSUs), the operational units deployed in the field. Each dataset provides household-level observations of target variables, together with

geographic identifiers at the first- or second-level administrative resolution.

Ethiopia Socioeconomic Survey 2018–2019 (ESS). We use the fourth wave of the Ethiopia Socioeconomic Survey (35), a nationally representative survey that collected information from 6,770 households between May and September 2019. We extract seven household-level variables: the average education level of adults, the logarithm of non-food expenditures, and estimates of apparent micronutrient intake for five micronutrients (iron, Folate (μg), Vitamin A (μg RAE), Vitamin B_{12} (μg), Zinc (mg)), extracted maintaining consistency with methods established in prior research (27, 36). After preprocessing, the analytical sample comprises 6,214 households distributed across 11 first-level administrative units.

Nigerian Living Standards Survey 2018–2019 (NLSS). We use the Nigerian Living Standards Survey (37), a nationally representative survey that collected information from 22,587 households between September 2018 and September 2019. We extract the same seven variables as for the ESS (27, 36). The analytical sample comprises 22,106 households distributed across 37 first-level administrative resolution units.

Sri Lanka Household Income and Expenditure Survey 2019 (HIES). We use the Sri Lanka HIES 2019 (38), which was conducted over 12 months to capture seasonal variation, with a total sample size of 25,000 housing units. Sri Lanka comprises 9 first-level administrative divisions and 25 second-level administrative divisions. We extract seven household-level variables: the average education level of members aged 17 or older, the logarithm of household income, and apparent intake for five key micronutrients, as for the ESS and NLSS (27, 36).

Sri Lanka Vulnerability Analysis and Mapping survey 2024 (VAM). We use the WFP Vulnerability Analysis and Mapping survey for Sri Lanka (5, 39), which randomly selects 600 households per district for a total of 15,000 households across 25 districts. We extract six variables: an education score (average of the fraction of adults with higher education and the fraction of children attending school), the logarithm of household income, the reduced Coping Strategies Index (rCSI), the Food Consumption Score (FCS), the Food Expenditure Share (FES), and space per person (number of rooms divided by household size).

Yemen mobile Vulnerability Assessment and Mapping 2025 (mVAM). We use the Yemen mVAM dataset collected between August 2025 and January 2026 (40), gathered by WFP through daily Computer Assisted Telephone Interviews. The analytical dataset contains 54,702 observations from 44,675 distinct households, distributed across 22 first-level administrative resolution units and 331 second-level administrative resolution units. We extract three variables: the logarithm of total monthly per-person expenditures, the rCSI, and the FCS.

Mozambique Post-Shock Food Security Assessment 2023. We use the Mozambique Post-Shock Food Security Assessment (41), which covers 11,080 households across 11 first-level administrative resolution units and 72 second-level administrative resolution units. We extract four variables: the FCS, the rCSI, and two composite scores representing the weekly frequency of consumption of vitamin A-rich and protein-rich each based on household-reported days of consumption in the preceding week (range 0–7).

Nigeria Multiple Indicator Cluster Survey (MICS). We use the Nigeria Multiple Indicator Cluster Survey 2021, Round 6 (6), conducted jointly by the National Bureau of Statistics and UNICEF. The survey sampled 41,532 households across 37 states, of which 39,632 households were successfully interviewed, together with 38,806 women and 17,347 men aged 15–49. Nigeria comprises 37 first-level administrative units. We extract three household-level variables: the average adult education level, space per person, and a composite wealth score.

Zimbabwe Multiple Indicator Cluster Survey (MICS). We use the Zimbabwe Multiple Indicator Cluster Survey 2019, Round 6 (42), conducted by the Zimbabwe National Statistics Agency with support from UNICEF. A total of 12,012 households were selected across 462 clusters; 11,091 households were successfully interviewed. The survey was designed to provide estimates at the national level and for ten provinces: Bulawayo, Manicaland, Mashonaland Central, Mashonaland East, Mashonaland West, Matabeleland North, Matabeleland South, Midlands, Masvingo, and Harare. We extract three household-level variables: the average adult education level, space per person, and a composite wealth score.

Contextual features

We incorporate continuous contextual features that capture environmental and socioeconomic conditions expected to explain sub-national variation in the target variables. All features are matched to household locations using the finest available spatial resolution and are treated as exogenous predictors throughout. We also incorporate a categorical feature describing the settlement sector of a given household.

Market accessibility. We use estimated travel time to the nearest market or urban centre, computed at high spatial resolution from road-network and land-cover data (28). This variable captures remoteness as a proxy for access to food markets and services.

Relative Wealth Index (RWI) and wealth indicator (*wscore*). We use the RWI derived from de-identified mobile-phone connectivity data and satellite imagery (26). The index provides a continuous measure of relative household wealth at sub-kilometre resolution. For Yemen, the relative wealth index dataset was not available, so we substituted it with a wealth indicator *wscore* coming from the most recent MICS survey, available at the first administrative level.

Environmental indicators. We incorporate the Normalised Difference Vegetation Index (NDVI), land surface temperature, and precipitation summaries aggregated over relevant seasonal windows (29). These variables capture agro-climatic conditions that influence food production and dietary outcomes, and are included primarily for datasets containing micronutrient intake targets.

Sector. The sector variable identifies the settlement or survey-sector category associated with each observation. In all datasets, sector distinguishes rural from urban areas; in the Sri Lankan surveys, an additional estate sector is also included, reflecting the country-specific sampling structure. This variable captures broad differences in population setting that are part of the survey design and may be associated with differences in livelihoods, infrastructure, market access, and household characteristics.

Conditional normalizing flow model

We model $p(Y | X)$ using conditional normalizing flows (cNF). A normalizing flow defines an invertible, differentiable mapping $f_\theta : \mathbb{R}^d \rightarrow \mathbb{R}^d$ from the target space to a latent space with a tractable base distribution p_Z (here, a standard multivariate normal). Conditioning on X is incorporated by making the parameters of each coupling layer a function of X :

$$Z = f_\theta(Y; X), \quad (2)$$

with conditional likelihood

$$\log p(Y | X) = \log p_Z(f_\theta(Y; X)) + \log \left| \det \frac{\partial f_\theta}{\partial Y} \right|. \quad (3)$$

Model parameters θ are estimated by maximising the conditional log-likelihood over the observed training data. At inference time, synthetic samples for region a_ℓ are generated by drawing $Z \sim p_Z$ and applying the inverse transformation conditioned on the contextual features X_{a_ℓ} associated with that region:

$$Y = f_\theta^{-1}(Z; X_{a_\ell}). \quad (4)$$

We use the publicly available implementation in the Python library `probaforms` (43).

Context-conditioned variant (cNF). In the primary setting, the model is conditioned on the full set of contextual features available for a given dataset, as described in the previous section. The sector condition is one-hot encoded and attached to the continuous part of the conditional input. These features provide the information used to refine sub-national distributions beyond what is available in the sparse observed sample.

Region-conditioned variant (NF). To isolate the contribution of continuous context variables, we consider a reduced model conditioned only on a one-hot encoding of the first-level administrative resolution region label. This variant retains spatial grouping but removes all exogenous contextual features, allowing a direct assessment of how much of the improvement is attributable to informative conditioning versus the sole region of belonging identification.

Baselines

In different parts of this work, we compare the cNF and NF models to three reference methods.

Oversampling. For each held-out record, the oversampling baseline draws a target vector with replacement from the pooled national sparse subsample, ignoring all contextual covariates and regional labels. In the main comparison to cNF, oversampling is evaluated at the ADM1 level after matching the held-out sample size. Because the resampling pool is the entire national subsample and no conditioning information is used, every region receives draws from the same national distribution. This baseline serves as the primary reference for evaluating whether the generative framework leveraging exogenous information can outperform structured resampling.

National sample baseline. Regional distributions are approximated by assigning the same national-level distribution from the subsample to all regions, thereby ignoring any sub-national heterogeneity. This baseline serves to assess whether the conditional generative model provides meaningful improvements for small-area estimation.

Bayesian multivariate linear baseline. In the context of small-area estimates, we use this baseline to assess the performance of our method for aggregate statistics, specifically average estimates. We implement a multivariate Bayesian linear regression with a flat prior. Let $Y_i \in \mathbb{R}^q$ denote the vector of target variables for observation i , and $X_i \in \mathbb{R}^p$ the corresponding vector of conditioning features (plus an intercept term). The model is specified as:

$$Y_i = X_i^\top \beta + \epsilon_i, \quad \epsilon_i \sim \mathcal{N}(0, \Sigma),$$

where $\beta \in \mathbb{R}^{p \times q}$ is the matrix of regression coefficients and $\Sigma \in \mathbb{R}^{q \times q}$ is the residual covariance matrix. Under a flat prior on β , the posterior mean coincides with the ordinary least squares estimator $\hat{\beta} = (X^\top X)^{-1} X^\top Y$, and the residual covariance is estimated as $\hat{\Sigma} = \frac{1}{n-p} (Y - X\hat{\beta})^\top (Y - X\hat{\beta})$. For a new input X_i , the posterior predictive distribution for the target variable i is given by:

$$\mathcal{N}(\hat{\mu}_i, \text{diag}(\hat{\Sigma}_i)),$$

where $\hat{\mu}_i = X_i^\top \hat{\beta}$ and $\hat{\Sigma}_i = (1 + h_i) \text{diag}(\hat{\Sigma})$, with $h_i = X_i^\top (X^\top X)^{-1} X_i$ denoting the leverage term. For each conditioning vector, the Bayesian model produces a Gaussian posterior predictive distribution characterised by a mean $\hat{\mu}_i$ and standard deviation $\sqrt{\text{diag}(\hat{\Sigma}_i)}$. Because the model assumes Gaussian outcomes, these two quantities fully characterise the predictive distribution. Regional

mean estimates are obtained by averaging posterior predictive means across all observations belonging to a given first-level administrative unit; regional uncertainties are obtained analogously from the posterior predictive variances. We compare the resulting regional mean estimates to those obtained from the cNF-generated data and from the ground-truth survey. The Bayesian model provides probabilistic estimates of regional means but does not generate household-level synthetic observations. In contrast, cNF produces synthetic household-level data from which both aggregate indicators and full distributions can be derived.

Evaluation metrics

Earth Mover’s Distance (EMD). Distance between distributions is measured using the Earth Mover’s Distance (Wasserstein-1 distance) between the generated and true sub-national distributions. For two univariate distributions P and Q , $\text{EMD}(P, Q) = \int |F_P(x) - F_Q(x)| dx$, where F_P and F_Q are the respective CDFs. Lower EMD indicates higher distributional fidelity. Target variables are scaled by the interquartile range (IQR) of their full-dataset distribution prior to distribution evaluation, so that metrics are comparable across variables with different units and magnitudes. IQR scaling is preferred over standard-deviation scaling because several target variables, particularly expenditure and consumption measures, exhibit heavy tails for which the standard deviation is sensitive to extreme values. Note that EMD is therefore reported in IQR units, whereas MAE (below) is expressed in standard-deviation units; the two metrics are not on a common scale.

Mean Absolute Error (MAE) Aggregate accuracy is measured as the absolute difference between the estimated and true sub-national mean, expressed in units of the target variable’s standard deviation:

$$\text{MAE}_r = \frac{|\hat{\mu}_r - \mu_r|}{\sigma_Y}. \quad (5)$$

Improvement over baseline. To quantify improvement relative to oversampling, we define

$$\Delta = \text{Err}_{\text{baseline}} - \text{Err}_{\text{model}}, \quad (6)$$

where Err is either EMD or MAE. Positive Δ indicates that the model outperforms oversampling; $\Delta = 0$ corresponds to parity. Results are always averaged on random seeds.

Statistical tests

We use paired one-sided Wilcoxon signed-rank tests to compare model performance across dataset–target-variable pairs, where each pair contributes one observation averaged over regions and seeds. This test is used in Figure 2 (cNF vs. NF+sector vs. NF vs. oversampling) and Figure 6A (cNF vs. Bayesian baseline). For the spatial analysis in Figure 5, variable-level significance is assessed with one-sided paired t -tests across first-level administrative regions (averaged over seeds), with Benjamini–Hochberg false discovery rate (BH-FDR) correction applied across variables within each dataset. In the supplementary bias analysis (figure S3), group differences are assessed with two-sided Welch’s independent two-sample t -tests. All tests use $\alpha = 0.05$. Because multiple target variables within a dataset are not fully independent, the resulting p -values should be interpreted as descriptive measures of evidence rather than exact estimates under strict independence assumptions; the consistency of effects across datasets, targets, and evaluation metrics provides additional support for the robustness of the observed patterns.

Intrinsic sub-national variability

We measure intrinsic sub-national variability as the EMD between the true national distribution and the true first-level administrative resolution-level distribution. Regions with high intrinsic variability deviate substantially from the national average; those with low variability are well-approximated by the national subsample. This measure is used to assess the utility of cNF for small-area refinement in Figure 7.

Feature attribution via Shapley values

To assess the contribution of individual contextual variables to the improvement achieved by the fully context-informed cNF model, we compute Shapley values (44) for the performance gain Δ . In this analysis, Δ measures the added value of exogenous geospatial context relative to the NF+sector model, rather than relative to the oversampling baseline. We define $\Delta = Err_{NF+sector} - Err_{cNF}$, so that positive values indicate that adding the full set of contextual variables improves synthetic data quality beyond conditioning on sector alone. The Shapley baseline therefore includes sector conditioning: the decomposition isolates the added contribution of the exogenous continuous features, not their

total effect. For each combination of dataset, target variable, first-level administrative region, and random seed, the Shapley value of contextual feature group X_j is estimated by averaging the marginal change in Δ when X_j is included versus excluded, over all possible subsets of the remaining groups. Because only three contextual feature groups were considered, exact Shapley values were computed by evaluating all possible feature-group subsets; for each subset, a separate cNF model is retrained using only that subset of contextual feature groups (together with sector and region), so that Shapley contributions reflect the effect of each group on the learned conditional distribution rather than on inference-time masking or permutation. Shapley values are computed at the level of individual regions, target variables, and seeds, and are then averaged; uncertainty is reported as the standard error of the mean across regions and seeds. Positive Shapley values indicate contextual feature groups that increase the advantage of the fully context-informed cNF model over NF+sector, while negative values indicate groups whose inclusion reduces this advantage. Negative contributions can arise from collinearity among contextual feature groups, from measurement error in model-derived covariates, or from cases where a group introduces noise for a particular dataset–target combination rather than useful signal. For visualization, target variables are grouped into four broad domains. Food-consumption-related targets include the Food Consumption Score (FCS), Food Expenditure Share (FES), and reduced Coping Strategies Index (rCSI). Micronutrient-intake-related targets include iron (mg), folate (μg), vitamin A (μg retinol activity equivalents, RAE), vitamin B12 (μg), and zinc (mg), together with food-group indicators related to iron, protein, and vitamin A. Education-related targets include adult education and education score. Income- and expenditure-related targets include log expenditures, log per-capita expenditures, log income, wealth score, and space per person.

Decision support meta-model

To characterize when generative refinement is most beneficial, we trained a supplementary decision-tree model using region-level features as predictors. For each region, the input features were the intrinsic variability of the target distribution, measured as the mean discrepancy between the true regional ($l = 1$) and true national distributions, and the effective training sample size. We defined a binary target equal to 1 when the mean improvement, defined as the difference in EMD between

the baseline and the cNF was positive and 0 otherwise, and trained a `DecisionTreeClassifier` with balanced class weights, and hyperparameters were tuned via stratified 5-fold cross-validation. Classification performance was evaluated using ROC–AUC. This setup evaluates whether a simple interpretable model can predict, based solely on sample size and intrinsic variability, when cNF refinement is likely to yield more accurate distributions than the national subsample baseline on datasets that are scarce to begin with.

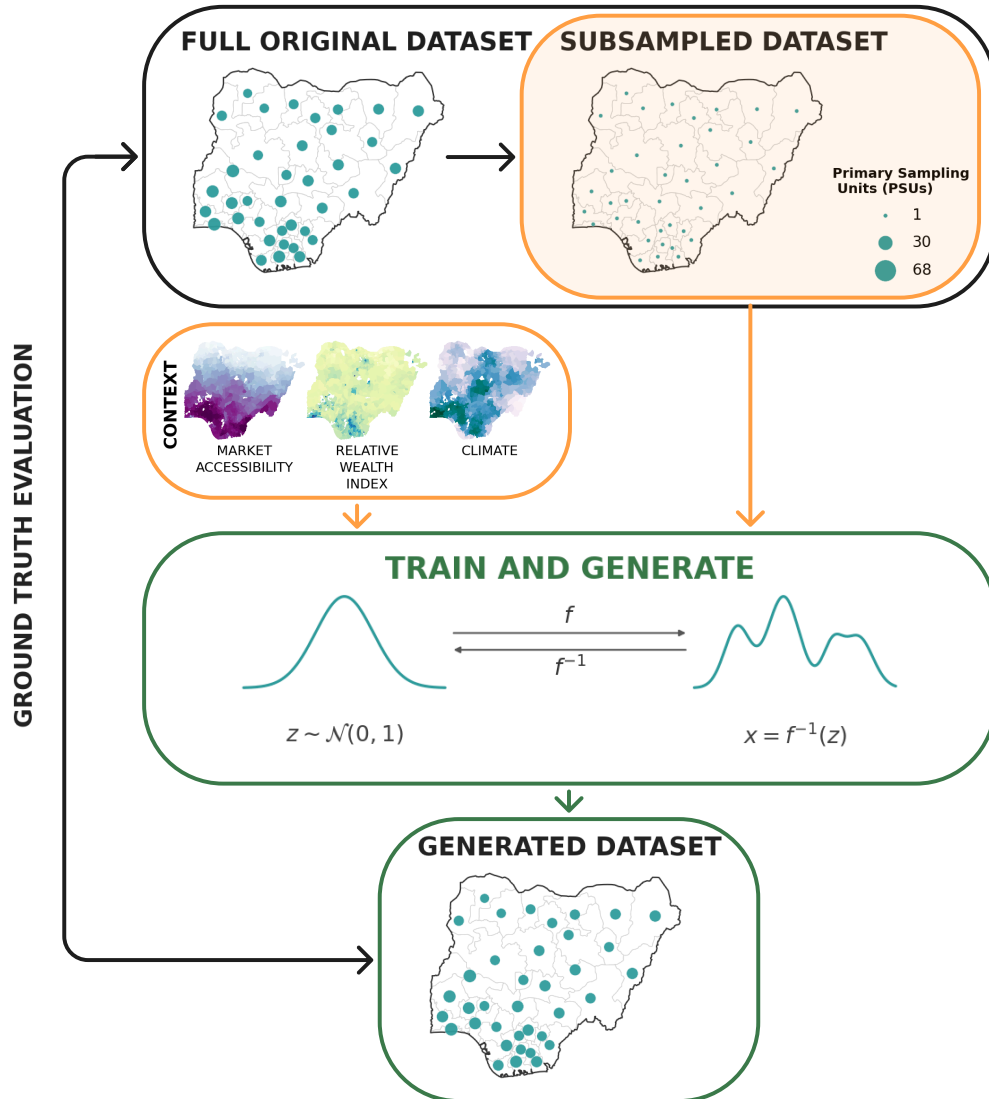


Figure 1: Proposed framework on the illustrative example of Nigeria. We simulate data scarcity by keeping only one survey cluster per region, train a generative AI model conditioned on contextual features, generate synthetic data for excluded locations, and compare them with held-out survey data for evaluation.

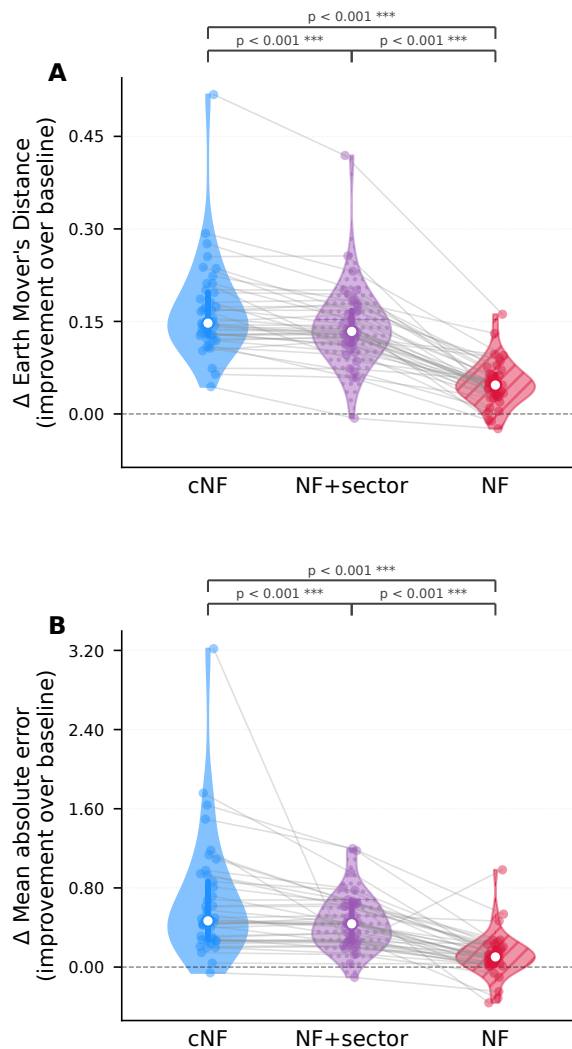


Figure 2: Context-informed generative models outperform oversampling in generating sub-national data. Each point represents a target variable in a dataset, averaged over random seeds and first-level administrative regions. Points are connected across conditioning strategies: full geospatial context (cNF, blue), categorical region and sector (NF+sector, purple), and region only (NF, red). The y-axis shows improvement over oversampling, $\Delta = Err_{oversampling} - Err_{model}$, so positive values indicate better performance. **(A)** Earth Mover's Distance (EMD) measures distributional similarity on IQR scaled variables; **(B)** Mean Absolute Error (MAE) measures sub-national mean accuracy in standard-deviation units. Brackets show paired one-sided Wilcoxon signed-rank tests.

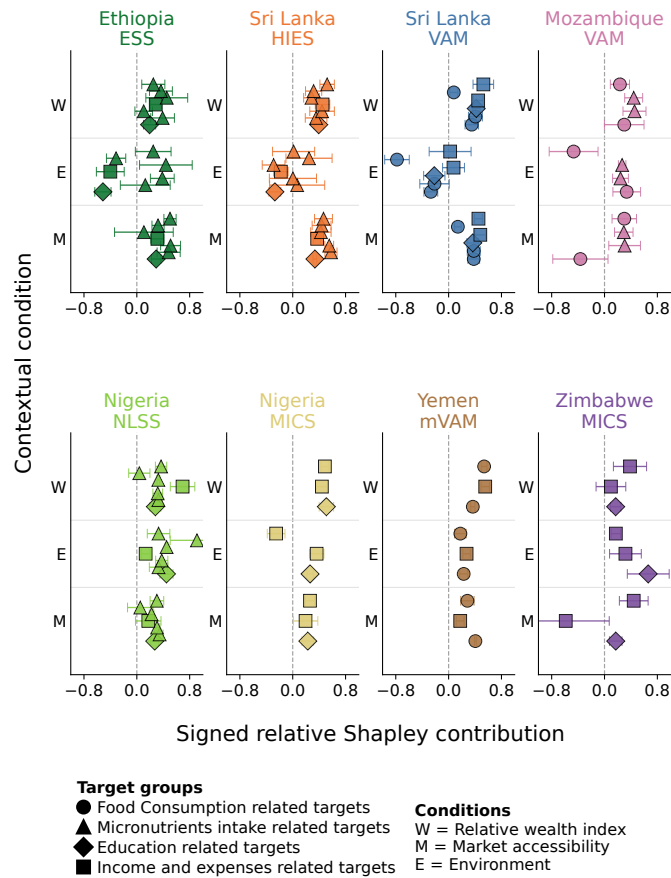


Figure 3: Shapley-based relative contribution of contextual feature groups to synthetic data quality. The figure reports signed relative Shapley contributions for each of three contextual feature groups — relative wealth (W), market accessibility (M), and environment (E) — across survey datasets and countries. All $2^3 = 8$ subsets are enumerated exhaustively, with a separate cNF model retrained for each subset. Raw Shapley values were normalized by the total absolute Shapley contribution. Points indicate average signed relative Shapley contributions over seeds and first-level administrative units, while horizontal error bars indicate standard errors scaled by the same factor. The vertical dashed line marks zero contribution: values to the right indicate a positive relative contribution to the quality metric, while values to the left indicate a negative relative contribution. Marker shapes distinguish broad groups of outcome variables: food consumption, micronutrient intake, education, and income or expenditure. The specific outcome variables included in each group are reported in the Methods.

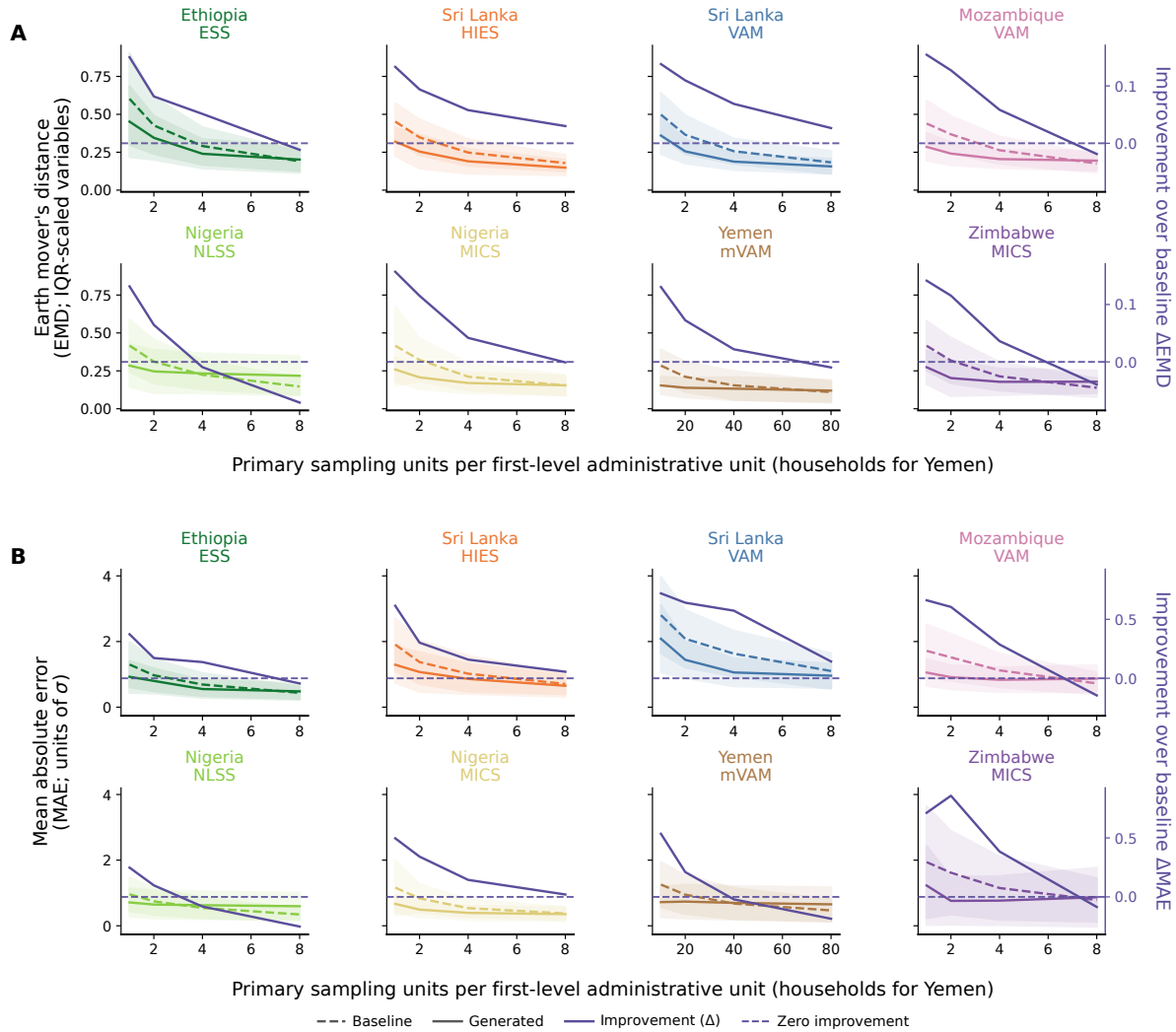


Figure 4: Sensitivity analysis of generated data quality to training sample size. (A) Earth Mover’s Distance (EMD) computed on IQR-scaled variables. (B) Mean Absolute Error (MAE) in units of σ . Solid colored lines show the generated model error and dashed colored lines show the oversampling baseline, averaged across variables, first-level administrative units, and random seeds; shaded areas indicate one standard deviation. The secondary y-axis reports improvement over the baseline, defined as $\Delta = Err_{\text{baseline}} - Err_{\text{generated}}$. The horizontal dashed line marks zero improvement, with positive values indicating better performance than the baseline. Training sample size denotes primary sampling units per first-level administrative unit, except for Yemen, where it denotes households.

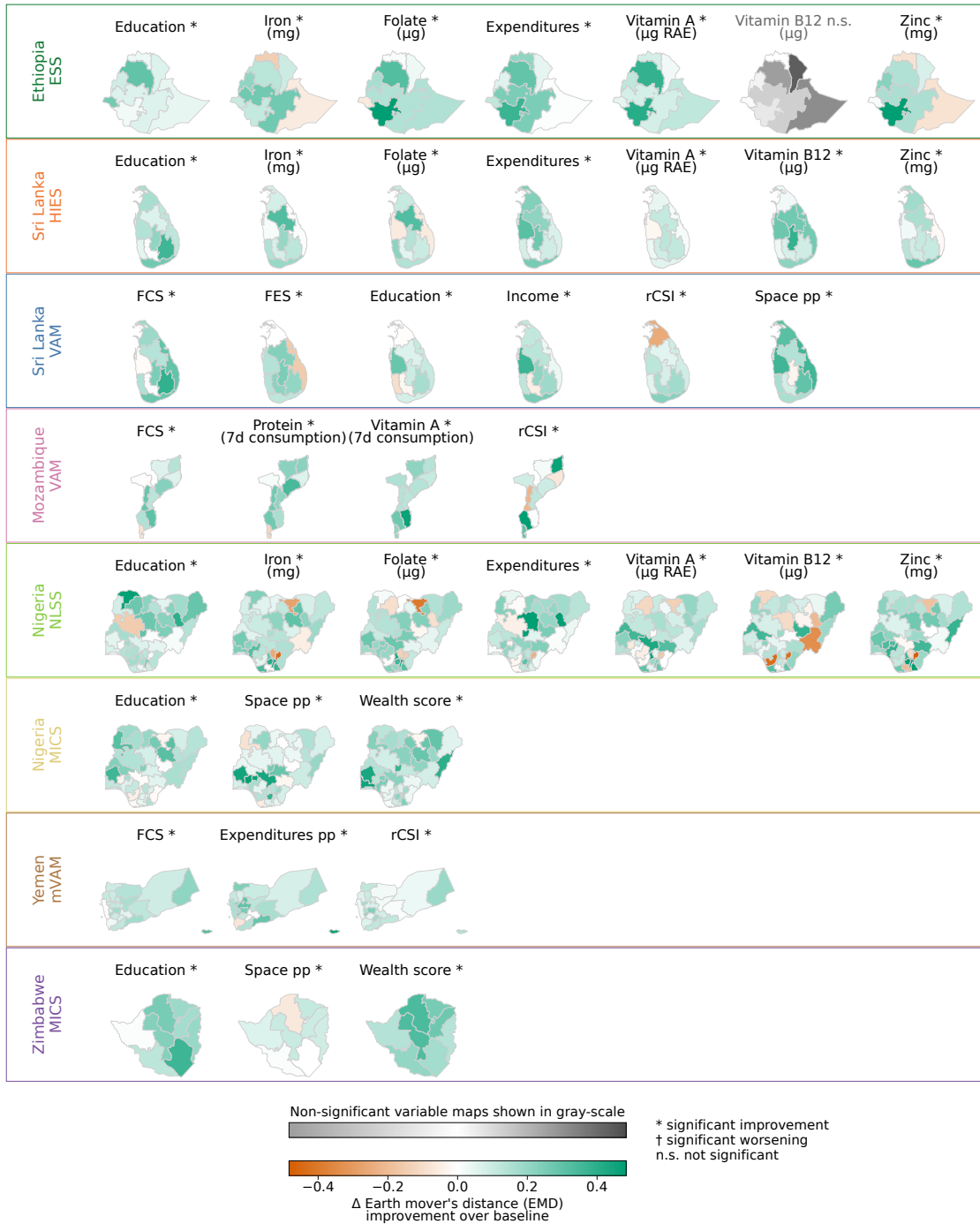


Figure 5: Spatial heterogeneity in distribution refinement. Maps show Δ EMD between the oversampling baseline and the cNF model at first-level administrative resolution, on IQR-scaled variables and averaged over seeds. Positive values indicate better cNF performance; negative values indicate better oversampling performance. Coloured maps indicate variables with significant improvement, tested with a one-sided paired t -test across regions and BH-FDR correction; non-significant variables are shown in greyscale. Symbols denote significant improvement (*), significant worsening (†), and non-significance (n.s.).

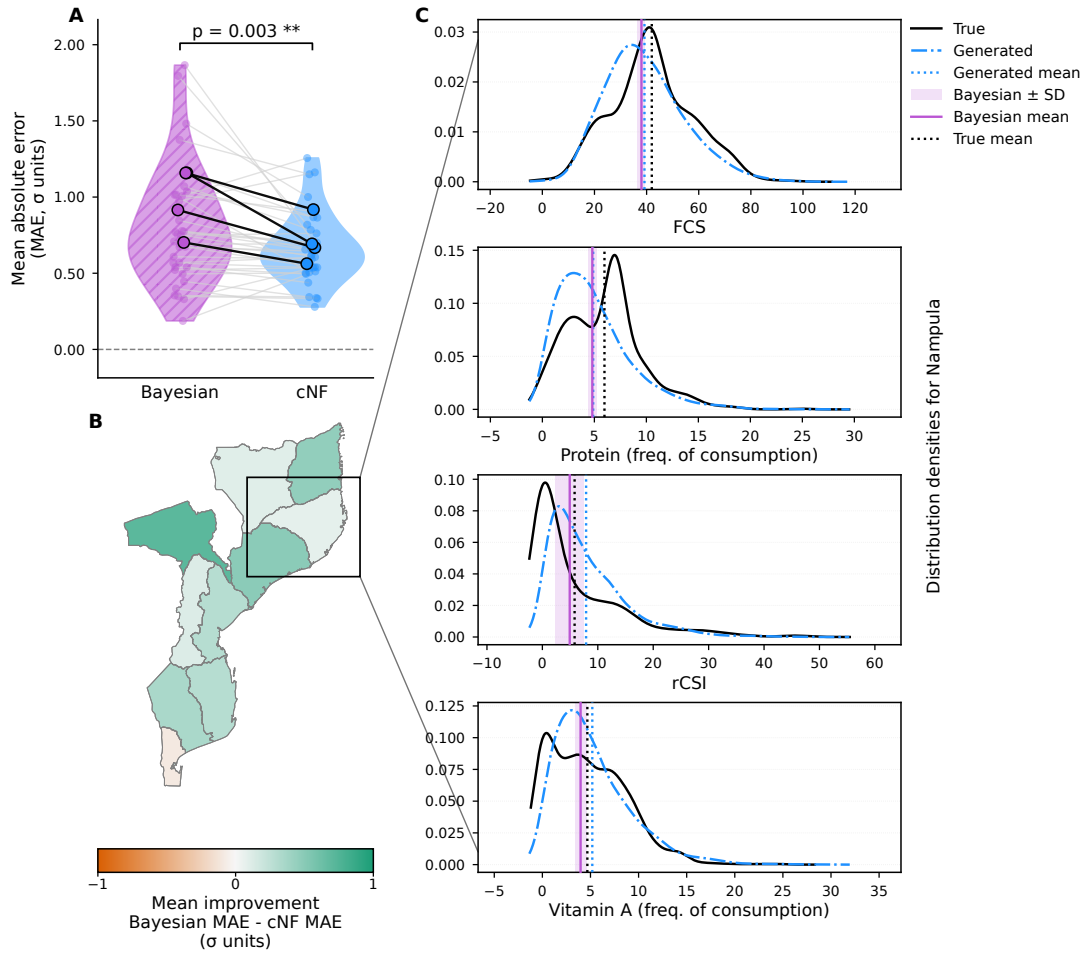


Figure 6: Aggregate mean-error comparison and local distributional diagnostics. (A) Mean absolute error (MAE) of the Bayesian multivariate linear baseline and the context-conditioned normalizing flow (cNF), expressed in target-variable standard deviation units. Each connected pair represents one dataset–target-variable combination; highlighted pairs correspond to the Mozambique VAM variables shown in panels B and C. The bracket shows a paired one-sided Wilcoxon signed-rank test. Because the Bayesian baseline predicts sub-national means, the comparison is limited to aggregate MAE. (B) Mozambique VAM first-level administrative-unit map. Colours show mean improvement of cNF over the Bayesian baseline across target variables, $\Delta = \text{MAE}_{\text{Bayesian}} - \text{MAE}_{\text{cNF}}$, with positive values indicating lower error for cNF. The boxed region identifies Nampula. (C) Household-level distributions for Nampula. Curves compare true empirical and cNF-generated distributions; vertical lines and shading show the true mean, generated mean, Bayesian posterior mean, and Bayesian posterior uncertainty. The panels link aggregate performance to local distributional diagnostics, which are available because cNF generates household-level records.

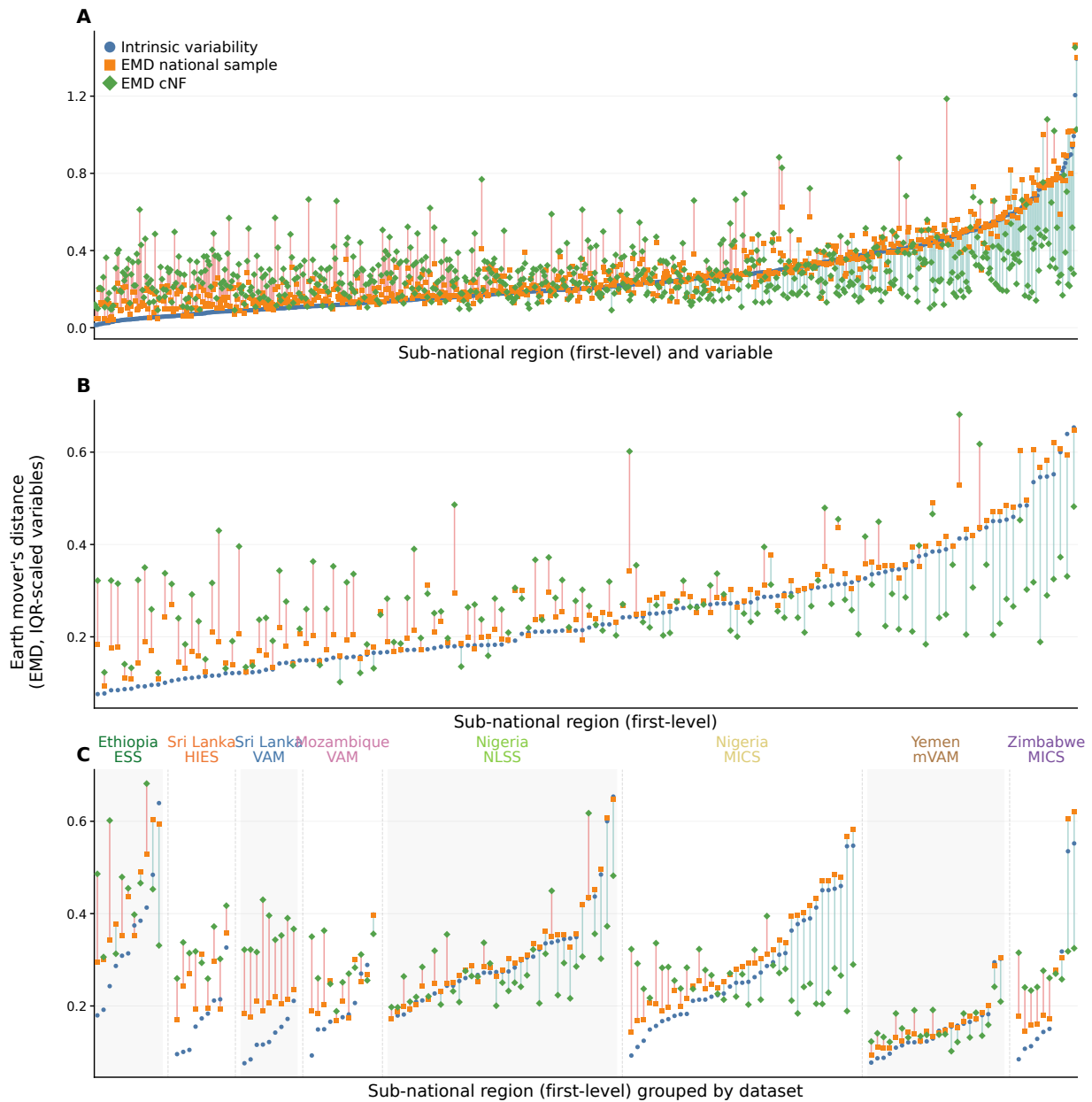


Figure 7: Context-conditioned normalizing flow improves sub-national estimates when regional variability is high. Points show Earth Mover's Distance (EMD), averaged over seeds. In panel A, each point corresponds to one variable in one first-level administrative unit; in panels B and C, values are also averaged over variables. Blue circles indicate intrinsic variability in the true data, orange squares the national subsample baseline, and green diamonds the cNF-generated data. Vertical connectors are blue when cNF improves over the baseline and red otherwise. **A:** regions and variables ordered by intrinsic variability. **B:** regions averaged over variables and ordered by intrinsic variability. **C:** same regions grouped by dataset.

References and Notes

1. C. Elbers, J. O. Lanjouw, P. Lanjouw, Micro-Level Estimation of Poverty and Inequality. *Econometrica* **71** (1), 355–364 (2003), doi:10.1111/1468-0262.00399.
2. J. Wakefield, *et al.*, Estimating under-five mortality in space and time in a developing world context. *Statistical Methods in Medical Research* **28** (9), 2614–2634 (2019), doi:10.1177/0962280218767988.
3. R. E. Fay III, R. A. Herriot, Estimates of income for small places: an application of James-Stein procedures to census data. *Journal of the American Statistical Association* **74** (366a), 269–277 (1979).
4. G. E. Battese, R. M. Harter, W. A. Fuller, An error-components model for prediction of county crop areas using survey and satellite data. *Journal of the American Statistical Association* **83** (401), 28–36 (1988).
5. World Food Programme, Food Security Assessments (2025), <https://vamresources.manuals.wfp.org/docs/food-security-assessments>, published 2025-08-12, updated 2025-10-10, accessed 2026-04-01.
6. National Bureau of Statistics (Nigeria), United Nations Children’s Fund (UNICEF), *Nigeria Multiple Indicator Cluster Survey and National Immunization Coverage Survey 2021*, Survey findings report, United Nations Children’s Fund (UNICEF), New York, USA (2022), <https://11nq.com/f9hy44k>.
7. S. Bourou, A. El Saer, T. H. Velivassaki, A. Voulkidis, T. Zahariadis, A Review of Tabular Data Synthesis Using GANs on an IDS Dataset. *Information* **12** (9), 375 (2021), doi:10.3390/info12090375, <https://www.mdpi.com/2078-2489/12/9/375>.
8. Z. Wang, *et al.*, A Comprehensive Survey on Data Augmentation. *arXiv preprint arXiv:2405.09591* (2024), doi:10.48550/arXiv.2405.09591, <https://arxiv.org/abs/2405.09591>.

9. L. Xu, M. Skoularidou, A. Cuesta-Infante, K. Veeramachaneni, Modeling Tabular Data using Conditional GAN. *arXiv preprint arXiv:1907.00503* (2019), doi:10.48550/arXiv.1907.00503, <https://arxiv.org/abs/1907.00503>.
10. A. X. Wang, B. P. Nguyen, TTVAE: Transformer-based generative modeling for tabular data generation. *Artificial Intelligence* **340** (C), 104292 (2025), doi:10.1016/j.artint.2025.104292, <https://doi.org/10.1016/j.artint.2025.104292>.
11. D. J. Rezende, S. Mohamed, Variational Inference with Normalizing Flows, in *Proceedings of the 32nd International Conference on Machine Learning (ICML)*, F. Bach, D. Blei, Eds. (PMLR), vol. 37 of *Proceedings of Machine Learning Research* (2015), pp. 1530–1538, <https://proceedings.mlr.press/v37/rezende15.html>.
12. L. Dinh, J. Sohl-Dickstein, S. Bengio, Density estimation using Real-NVP, in *International Conference on Learning Representations (ICLR)* (2017).
13. C. Durkan, A. Bekasov, I. Murray, G. Papamakarios, Neural spline flows. *Advances in Neural Information Processing Systems* **32** (2019).
14. Y. Jiang, S. Liang, J. Choi, Synthetic Survey Data Generation and Evaluation, in *Proceedings of the 31st ACM SIGKDD Conference on Knowledge Discovery and Data Mining, KDD '25* (ACM) (2025), pp. 2292–2302, doi:10.1145/3690624.3709421, <https://dl.acm.org/doi/10.1145/3690624.3709421>.
15. T. Liu, Z. Qian, J. Berrevoets, M. van der Schaar, GOGGLE: Generative Modelling for Tabular Data by Learning Relational Structure, in *Proceedings of the International Conference on Learning Representations (ICLR)* (2023), <https://openreview.net/forum?id=goggle-iclr2023>, poster Presentation.
16. S. Y. Lim, H. Yun, P. Bansal, D.-K. Kim, E.-J. Kim, A Large Language Model for Feasible and Diverse Population Synthesis. *arXiv preprint arXiv:2505.04196* (2025), submitted to Transportation Research Part C: Emerging Technologies, doi:10.48550/arXiv.2505.04196, <https://doi.org/10.48550/arXiv.2505.04196>.

17. M. Johnsen, O. Brandt, S. Garrido, F. Pereira, Population synthesis for urban resident modeling using deep generative models. *Neural Computing and Applications* **34**, 4677–4692 (2022), doi: 10.1007/s00521-021-06634-7, <https://doi.org/10.1007/s00521-021-06634-7>.
18. R. Tanton, K. Edwards, *Spatial Microsimulation: A Reference Guide for Users*, vol. 6 (Springer Science & Business Media) (2012).
19. D. Liu, *et al.*, Synthetic Data Generation for Augmenting Small Samples. *arXiv preprint arXiv:2501.18741* (2025).
20. D. Manousakas, S. Aydöre, On the Usefulness of Synthetic Tabular Data Generation. *arXiv preprint arXiv:2306.15636* (2023), data-centric Machine Learning Research (DMLR) Workshop at the 40th International Conference on Machine Learning (ICML), <https://doi.org/10.48550/arXiv.2306.15636>.
21. I. Shumailov, *et al.*, AI models collapse when trained on recursively generated data. *Nature* **631**, 755–759 (2024), doi:10.1038/s41586-024-07566-y.
22. J. Jordon, *et al.*, *Synthetic Data – what, why and how?*, Tech. rep., The Royal Society (2022), <https://arxiv.org/abs/2205.03257>, arXiv:2205.03257.
23. Materials and methods are available as supplementary material.
24. N. Jean, *et al.*, Combining satellite imagery and machine learning to predict poverty. *Science* **353** (6301), 790–794 (2016), doi:10.1126/science.aaf7894.
25. C. Yeh, *et al.*, Using publicly available satellite imagery and deep learning to understand economic well-being in Africa. *Nature Communications* **11** (1), 2583 (2020).
26. G. Chi, H. Fang, S. Chatterjee, J. E. Blumenstock, Microestimates of wealth for all low- and middle-income countries. *Proceedings of the National Academy of Sciences* **119** (3), e2113658119 (2022).
27. V. Voukelatou, *et al.*, Predicting risk of inadequate micronutrient intake with transferable machine learning models. *Scientific Reports* **16**, 4104 (2026), doi:10.1038/s41598-025-26179-7.

28. R. Benassai-Dalmau, *et al.*, Unequal journeys to food markets: Continental-scale evidence from open data in Africa. *arXiv preprint arXiv:2505.07913* (2025).
29. S. Huang, L. Tang, J. P. Hupy, Y. Wang, G. Shao, A commentary review on the use of normalized difference vegetation index (NDVI) in the era of popular remote sensing. *Journal of forestry research* **32** (1), 1–6 (2021).
30. C. Winkler, D. E. Worrall, E. Hoogeboom, M. Welling, Learning Likelihoods with Conditional Normalizing Flows. *arXiv preprint arXiv:1912.00042* (2019), doi:10.48550/arXiv.1912.00042, <https://arxiv.org/abs/1912.00042>.
31. M. S. M. Sajjadi, O. Bachem, M. Lucic, O. Bousquet, S. Gelly, Assessing Generative Models via Precision and Recall. *arXiv preprint arXiv:1806.00035* (2018), neurIPS 2018, <https://doi.org/10.48550/arXiv.1806.00035>.
32. H. Shimodaira, Improving predictive inference under covariate shift by weighting the log-likelihood function. *Journal of Statistical Planning and Inference* **90** (2), 227–244 (2000), doi:10.1016/S0378-3758(00)00115-4.
33. M. Agarwal, *et al.*, General Geospatial Inference with a Population Dynamics Foundation Model. *arXiv preprint arXiv:2411.07207* (2024), <https://arxiv.org/abs/2411.07207>.
34. World Food Programme, *WFP Document WFP-0000168485*, Tech. rep., World Food Programme (WFP) (n.d.), <https://docs.wfp.org/api/documents/WFP-0000168485/download/>, accessed: 2026-02-05.
35. Central Statistics Agency of Ethiopia, Ethiopia - Socioeconomic Survey 2018-2019 (ESS 2018/19) (2020), <https://microdata.worldbank.org/index.php/catalog/3823>, world Bank Microdata Library.
36. K. Tang, *et al.*, Modeling food fortification contributions to micronutrient requirements in Malawi using Household Consumption and Expenditure Surveys. *Annals of the New York Academy of Sciences* **1508** (1), 105–122 (2022).

37. N. B. of Statistics (Nigeria), Nigeria - Living Standards Survey 2018-2019 (NLSS 2018/19) (2021), <https://microdata.worldbank.org/index.php/catalog/3827>, world Bank Microdata Library.
38. Department of Census and Statistics (Sri Lanka), Sri Lanka - Household Income and Expenditure Survey 2019 (HIES 2019) (2023), <https://catalog.ihsn.org/catalog/11323>, iHNS Survey Catalog (World Bank Microdata ecosystem).
39. World Food Programme, WFP Vulnerability Analysis and Mapping (VAM) – Sri Lanka (data portal) (2021), <https://dataviz.vam.wfp.org/asia-and-the-pacific/sri-lanka/overview>.
40. World Food Programme, The World Food Programme’s Real-Time Monitoring Systems: Approaches and Methodologies, https://executiveboard.wfp.org/document_download/WFP-135070 (2021), accessed 2026-04-01.
41. World Food Programme, Annual country reports – Mozambique – 2023, MZ02 (2023), <https://www.wfp.org/publications/annual-country-reports-mozambique>, access the 2023 Mozambique Annual Country Report (operation MZ02) via the “View” entry on this page.
42. Zimbabwe National Statistics Agency (ZIMSTAT), United Nations Children’s Fund (UNICEF), *Zimbabwe 2019 Multiple Indicator Cluster Survey: Survey Findings Report*, Survey findings report, Zimbabwe National Statistics Agency and UNICEF, Harare, Zimbabwe (2020), <https://www.unicef.org/zimbabwe/reports/zimbabwe-2019-mics-survey-findings-report>.
43. M. Hushchyn, probaforms: Synthetic data generation for tables (2023), <https://pypi.org/project/probaforms/>, MIT License. Release date: 2023-07-26.
44. S. M. Lundberg, S.-I. Lee, A unified approach to interpreting model predictions. *Advances in neural information processing systems* **30** (2017).

45. F. Sibilla, Code and data for: Context-conditioned generative models enable sub-national refinement of sparse humanitarian survey data, https://github.com/federicasibilla/cNF_HS (2025), accessed: 2025.
46. N. Patki, R. Wedge, K. Veeramachaneni, The Synthetic Data Vault, in *2016 IEEE International Conference on Data Science and Advanced Analytics (DSAA)* (IEEE) (2016), pp. 399–410, doi:10.1109/DSAA.2016.49.
47. SDV Developers, SDV: Synthetic Data Vault, <https://github.com/sdv-dev/SDV> (2023), accessed: 2025-10-01.
48. M.-D. Stoian, E. Giunchiglia, T. Lukasiewicz, A Survey on Tabular Data Generation: Utility, Alignment, Fidelity, Privacy, and Beyond. *arXiv preprint arXiv:2503.05954* (2025), <https://arxiv.org/abs/2503.05954>.

Acknowledgments

We would like to thank Frances Knight for the support and feedback, Jonas De Meyer for the support on extracting and interpreting the mVAM data, and Shehan Fernando for the support on interpreting the Household Income and Expenditure Survey 2019 (HIES 2019). We acknowledge the Department of Census and Statistics, Sri Lanka, for providing the Sri Lanka HIES 2019 dataset used in this analysis.

Funding: F.S., K.K., D.P., R.S., were funded by the Lagrange Fellowship at the ISI Foundation. V.V., D.Piov., and K.Koup. were supported by the Gates Foundation (INV-037325) through the Modelling & Mapping the Risk of Inadequate Micronutrient Intake (MIMI) project. K.K. additionally received support from the Spanish Agency for International Development Cooperation (AECID) via UNICEF’s Frontier Data Network.

Author contributions: All authors contributed to the review of the final draft and approved the manuscript. F.S. contributed to conceptualization, methodology, software, formal analysis, visualization, and writing of the original draft. V.V. contributed to conceptualization, formal analysis,

data curation, and writing of the original draft. D. Piovani, K. Koupparis, D. Paolotti and R.S. contributed to conceptualization and formal analysis. K. Kalimeri contributed to conceptualization, formal analysis, and writing of the original draft. All the authors have read and approved the final manuscript.

Competing interests: There are no competing interests to declare.

Data and materials availability: The code used to preprocess the data, train the models, reproduce the analyses, and generate the figures is available at (45). Publicly available survey datasets used in this study, including the Ethiopia ESS, Nigeria NLSS, Nigeria MICS, and Zimbabwe MICS datasets, can be obtained from their original data repositories, as cited in the References. The Sri Lanka HIES 2019 dataset and the WFP VAM datasets are subject to access restrictions and are available from the original data providers upon reasonable request and subject to their data-use agreements.

Supplementary materials

Materials and Methods

Supplementary Text

Figs. S1 to S4

Table S1

References (39-48)

Supplementary Materials for
Context-conditioned generative models enable sub-national
refinement of sparse humanitarian survey data

Federica Sibilla, Vasiliki Voukelatou*, Duccio Piovani, Kyriacos Koupparis, Daniela Paolotti,
Rossano Schifanella, Kyriaki Kalimeri*

*Corresponding author. Email: vasiliki.voukelatou@wfp.com, kyriaki.kalimeri@isi.it

This PDF file includes:

Materials and Methods

Supplementary Text

Figures S1 to S4

Table S1

Materials and Methods

Predicting target variables using random forest and contextual features

For each dataset and target variable, we assessed the degree to which the available contextual features carry predictive signal over sub-national mean values using a random forest regressor. For each dataset, the feature matrix \mathbf{X} consisted of the contextual features available for that dataset (the same features used to condition the generative model), and the target vector \mathbf{y} contained the sub-national mean values of the variable of interest, averaged across random seeds. Rows with missing or non-finite values in either features or target were excluded. Dataset–variable pairs with fewer rows than the number of features plus one were skipped to avoid degenerate cross-validation folds. Model performance was evaluated under leave-one-out cross-validation (LOO-CV): for each sub-national unit, a random forest (100 trees, maximum depth 3, fixed random seed) was trained on all remaining units and used to predict the held-out unit. Constraining tree depth to 3 limits overfitting in the small-sample regime typical of sub-national datasets. Predictions were collected across all folds and used to compute three summary metrics: the coefficient of determination (R^2), the mean relative error (MRE, defined as the mean of $|y_{\text{true}} - y_{\text{pred}}|/|y_{\text{true}}|$ over non-zero true values), and the relative root mean squared error (rRMSE, defined as RMSE divided by the mean absolute true value). R^2 was computed globally over all LOO predictions rather than averaged across folds, making it sensitive to both bias and variance of the predictions. A positive R^2 indicates that contextual features carry generalizable predictive signal beyond the global mean; negative values indicate that the LOO model performs worse than a mean predictor, which is common when sample sizes are small relative to the complexity of the covariate–target relationship. For the correlation analysis with generative model error, only dataset–variable pairs with $R^2 > 0$ were retained, as negative R^2 values reflect model failure rather than a meaningful measure of contextual informativeness.

Evaluation framework for model comparison

We evaluate the quality of synthetic data along two independent axes: *fidelity* and *originality*. Fidelity measures the statistical similarity between the true and synthetic populations; originality measures the ability of the synthetic data to generalize beyond the training sample and cover the true population manifold. These two axes are complementary: a model that simply copies training

records would achieve high fidelity but low originality, while a model that generates highly diverse but unrealistic records would achieve high originality at the cost of fidelity.

Fidelity metrics. We assess fidelity at three levels of increasing complexity: marginal, bivariate, and joint. All three use the Earth Mover’s Distance (Wasserstein-1 distance) as the underlying discrepancy measure, and all three are normalized to a $[0, 1]$ scale using dataset-specific reference baselines, so that scores are comparable across variables, variable sets, and datasets with different units and scales.

For each fidelity level $k \in \{\text{marginal, bivariate, joint}\}$, we define a normalized score as:

$$F_k = \frac{\text{EMD}_{\text{LB},k} - \text{EMD}_{\text{model},k}}{\text{EMD}_{\text{LB},k} - \text{EMD}_{\text{UB},k}}, \quad (\text{S1})$$

clipped to $[0, 1]$, where $\text{EMD}_{\text{model}}$ is the distance between the true and synthetic distributions, EMD_{UB} is the distance achieved by an upper-bound reference, and EMD_{LB} is the distance achieved by a lower-bound reference. A score of 1 indicates that the model matches the upper-bound reference; a score of 0 indicates that the model matches the lower bound. All EMD computations are performed on IQR-scaled variables to ensure comparability across variables with different units and magnitudes. Scores are computed separately for each random seed and then averaged across seeds.

The *upper-bound* reference is a bootstrap sample of the true dataset — the same number of rows drawn with replacement — which preserves the true distribution up to sampling noise and represents the best achievable fidelity given finite sample size. The *lower-bound* reference differs by fidelity level and is designed to represent a clearly inadequate synthetic dataset:

- *Marginal fidelity* evaluates each target variable independently. EMD is computed between the true and synthetic univariate distributions for each variable separately, then averaged across variables. The lower bound replaces every value with the global empirical mean of that variable, collapsing all distributional shape to a point mass and representing a dataset that preserves the global mean while destroying all within-variable variability.
- *Bivariate fidelity* evaluates all pairwise combinations of target variables. EMD is computed on the joint two-dimensional distribution of each pair, then averaged across all $\binom{d}{2}$ pairs,

where d is the number of target variables. The lower bound is constructed by independently resampling each variable from its own empirical marginal distribution (with replacement), which preserves the univariate marginals while destroying all pairwise dependence.

- *Joint fidelity* evaluates the full multivariate distribution over all d target variables simultaneously. EMD is computed on the joint d -dimensional distribution. The lower bound follows the same construction as for bivariate fidelity — independent resampling of each variable — preserving marginals while destroying all multivariate dependence.

Originality metric. Originality is measured as the recall of the true population by the synthetic data, following (31). Recall quantifies the fraction of true data points covered by the synthetic distribution and is therefore sensitive to gaps in the generated data rather than to distributional shape per se.

Concretely, for each sub-national region (first-level administrative resolution), we fit a standard scaler on the true data for that region and apply it to both the true and synthetic target vectors. We then build a k -d tree on the scaled synthetic points and, for each true point, query whether at least one synthetic neighbor exists within a fixed radius $r = 0.5$ in the scaled joint target space. Recall for that region is the fraction of true points that have at least one such neighbor:

$$\text{Recall}_a = \frac{1}{n_a} \sum_{i \in a} \mathbf{1} \left[\min_{j \in \tilde{a}} \|x_i - \tilde{x}_j\|_2 \leq r \right], \quad (\text{S2})$$

where n_a is the number of true households in region a , x_i are scaled true points, and \tilde{x}_j are scaled synthetic points within the same region. The overall recall is the weighted average across regions, with weights proportional to the number of true households in each region. This procedure is applied independently for each random seed, and reported values are means and standard deviations across the five seeds.

Models

We benchmark the conditional normalizing flow (cNF) against two widely used generative models for tabular data from the SDV library (46, 47): TVAE and CTGAN (9). All models are trained on the full cleaned training dataset for each experiment and generate a synthetic population of equal

size to the training set. All models use default hyperparameters as implemented in the respective libraries.

CTGAN. CTGAN (9) is a conditional generative adversarial network designed for tabular data. It uses a conditional generator that explicitly conditions on discrete columns through a training-by-sampling strategy, and applies mode-specific normalisation to handle the mixed-type and multi-modal marginal distributions that are common in tabular data. In our setting, the sector variable (rural/urban/estate) is treated as a discrete conditioning column through CTGAN’s native conditional sampling mechanism; all target variables are treated as continuous. CTGAN is otherwise trained unconditionally with respect to the contextual features.

TVAE. TVAE (9) is a variational autoencoder adapted for tabular data. It uses the same data transformation pipeline as CTGAN — including mode-specific normalisation for continuous variables and one-hot encoding for discrete columns — but replaces the adversarial training objective with an evidence lower bound (ELBO). TVAE is trained without explicit conditioning on contextual features and generates samples unconditionally from the learned latent space.

cNF. The conditional normalizing flow used in the benchmark follows the same architecture and hyperparameters as in the main analysis (probaforms implementation (43), default settings). Since generation requires conditioning inputs, we construct the conditional input matrix by sampling rows with replacement from the joint empirical distribution of contextual features observed in the training dataset, preserving the observed covariate structure without extrapolation beyond the training support.

Supplementary Text

Context predictive power and cNF performance

To examine whether the predictive informativeness of contextual features is associated with cNF performance on aggregate estimates, we correlated the LOO R^2 of the random forest with the mean absolute error of the generative model across dataset–variable pairs (aggregate average values). Figure S4 shows results for each individual target variable; from these, we kept only those where

context was predictive ($R^2 > 0$) for the following analysis. Figure S2 shows a negative correlation between R^2 and generative model error (Pearson= -0.47 , Spearman= -0.49 , $n = 19$); negative correlations indicate that higher ADM1-level predictability is associated with lower cNF error. This suggests that when contextual features carry a stronger predictive signal over sub-national means, the generative model tends to produce lower absolute aggregate error. Note that this analysis correlates context predictiveness with cNF error, not with cNF improvement over the oversampling baseline; it therefore characterises settings where cNF performs well in absolute terms, which need not coincide with settings where it offers the largest gains relative to simpler approaches. The correlation is moderate and based on a limited number of dataset–variable pairs, and we cannot rule out the possibility that other factors — including architectural regularization, distributional smoothing, or dataset-specific properties — contribute independently to model performance.

Effect of sampling bias on distributional estimates

Figure S3 examines how a systematic bias in the training subsample—specifically, sampling restricted to urban households—affects the EMD distributions of oversampling and cNF across variable types. For all variables pooled, cNF significantly outperforms oversampling under both biased and unbiased sampling ($p < 0.001$), while the difference between biased and unbiased sampling is not significant for either oversampling ($p = 0.058$) or cNF ($p = 0.149$). For socioeconomic variables—wealth, income or expenditures, education, and space per person—cNF significantly outperforms oversampling only under unbiased sampling ($p < 0.001$), whereas the difference under biased sampling is not significant ($p = 0.072$). Across sampling conditions, the biased–unbiased difference is significant for cNF ($p = 0.030$) but not for oversampling ($p = 0.062$), suggesting that when the sample systematically excludes rural households, the absolute error for sector-related socioeconomic targets increases in a way that contextual conditioning alone cannot fully compensate for. Importantly, the relative improvement of cNF over oversampling under biased sampling does not imply that cNF corrects the bias; both methods inherit the same biased support, and the comparison reflects differential performance within that regime.

Model comparison results

We benchmarked the cNF against two widely used generative models for tabular data synthesis, TVAE and CTGAN (9), implemented via the SDV library (46, 47). The comparison is framed around the two axes introduced above: fidelity, measuring how closely the synthetic distribution reproduces the true population, and originality, measuring how well the synthetic data covers the true population manifold beyond the training sample. Within the context of tabular data generation, evaluating synthetic data becomes a well-defined task only after specifying the purpose of generation (48). Our setting — augmenting small, non-representative samples drawn from a larger inaccessible population — places particular emphasis on originality: the ideal synthetic dataset covers the population manifold as broadly as possible without distorting the statistical properties of the true multivariate distribution (16).

Figure S4 summarises the results. Panel A shows that cNF achieves comparable or higher fidelity than CTGAN and TVAE across most experiments, on all three fidelity dimensions (marginal, bivariate, and joint). Panel B shows the fidelity–originality trade-off as a scatter plot: cNF tends to occupy the upper-right region of the space — combining high fidelity with high originality — more consistently than the two baselines. CTGAN and TVAE frequently achieve competitive fidelity but lower originality, suggesting that they reproduce the statistical properties of the training sample without generalizing as effectively to the broader population manifold.

The only systematic exception is the Zimbabwe MICS dataset, where CTGAN and TVAE outperform cNF on fidelity. We attribute this to the quasi-categorical nature of the target variables in that dataset (education level, space per person, and a discrete wealth score): both CTGAN and TVAE incorporate mode-specific normalisation and explicit handling of discrete-like distributions, which gives them a structural advantage when the outcome space is effectively discrete. The cNF, by contrast, is designed for continuous targets and does not model discreteness explicitly, leading to distributional mismatch on variables with few distinct values. This limitation is acknowledged in the main text and motivates future extensions to mixed-type outcome spaces.

Taken together, these results indicate that cNF produces synthetic data that is competitive with — and often superior to — state-of-the-art tabular generative models on both fidelity and originality, while additionally offering the conditioning mechanism that enables the sub-national distributional

refinement evaluated in the main analysis. The two benchmarked alternatives, lacking an explicit mechanism to incorporate spatial contextual features at generation time, cannot be straightforwardly applied to the inference task studied in this paper.

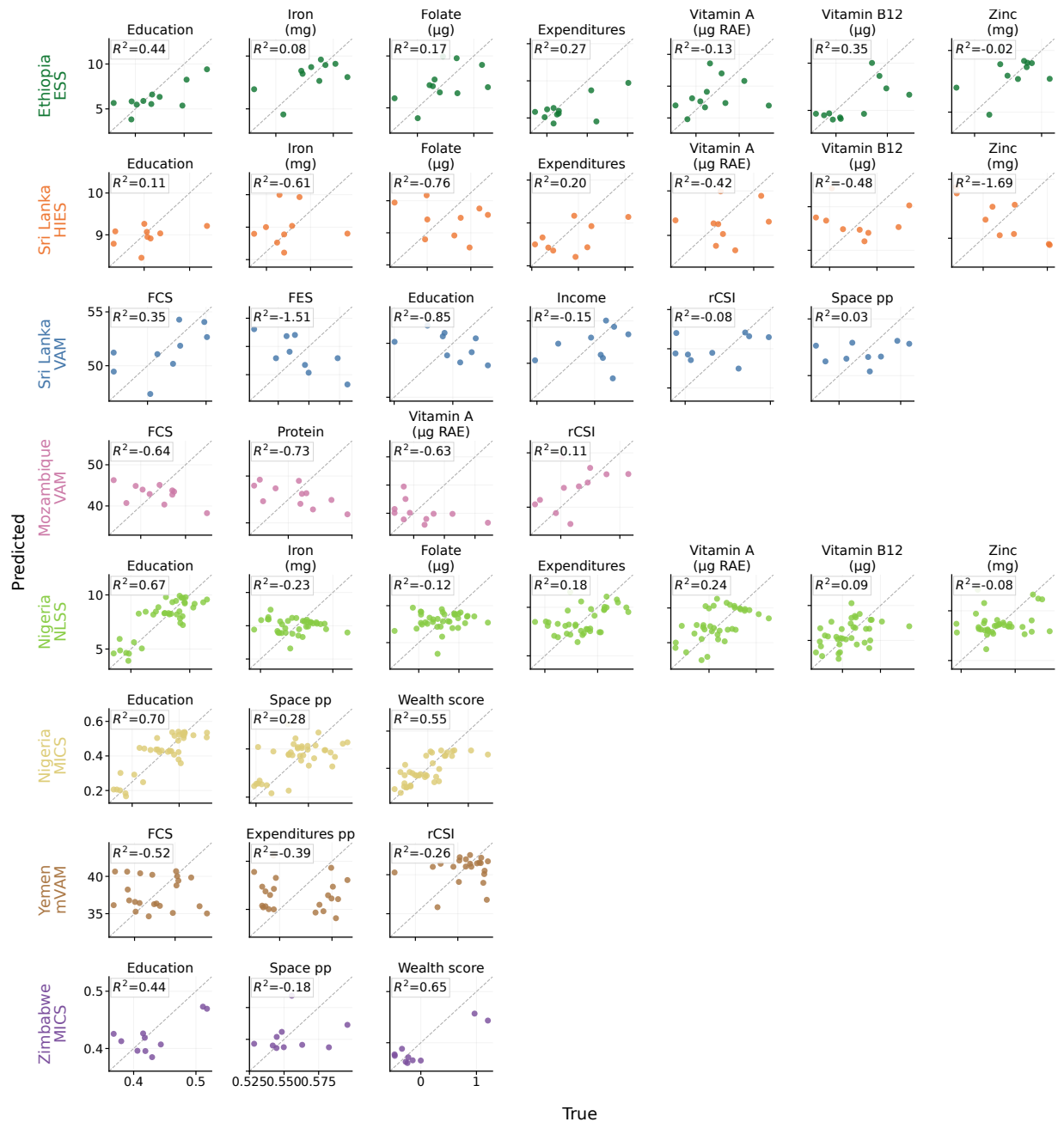


Figure S1: Leave-one-out random forest prediction of sub-national means. Scatter plots show leave-one-out predicted versus true sub-national mean values for each dataset and target variable. Each point represents one first-level administrative unit, and the dashed line indicates the identity line. Rows correspond to datasets and columns to target variables; rows with fewer target variables are left-aligned. The coefficient of determination (R^2) is reported in each panel and is computed across all leave-one-out predictions for the corresponding dataset–variable pair.

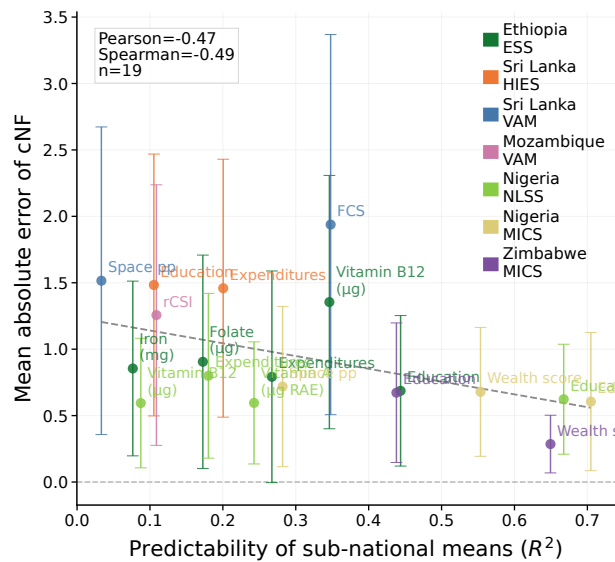


Figure S2: Contextual predictiveness and generative model error. Each point is a dataset–variable pair with positive LOO R^2 ($n=19$). The x-axis shows the R^2 of the random forest regressor trained on contextual features; the y-axis shows the mean absolute error of the generative model on sub-national mean estimates, with error bars indicating the standard deviation across sub-national units. Colors identify datasets. The dashed line is a linear fit. Pearson and Spearman correlations are shown in the inset.

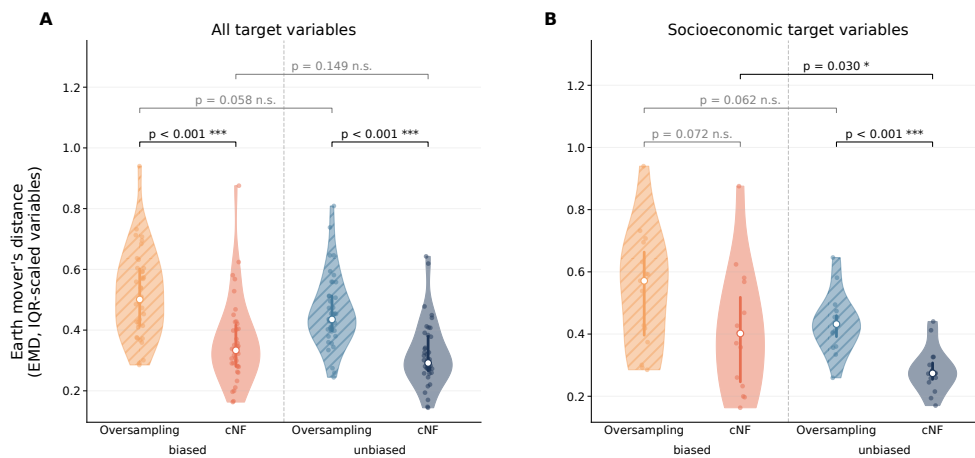


Figure S3: Urban-biased sampling increases absolute error but cNF remains beneficial under unbiased sampling. Each violin shows the distribution of Earth Mover's Distance (EMD) for oversampling and cNF under biased and unbiased national sub-sampling. In the biased condition, the sparse training sample is restricted to urban households; in the unbiased condition, the sparse training sample preserves the national urban–rural composition. Values are averaged over random subsampling seeds and first-level administrative regions for each dataset–target combination. **(A)** All target variables. **(B)** Socioeconomic target variables only: wealth, income or expenditures, education, and space per person. Brackets report two-sided Welch's independent two-sample tests. In panel A, cNF significantly outperforms oversampling under both biased and unbiased sampling ($p < 0.001$), while biased and unbiased sampling do not differ significantly for either oversampling ($p = 0.058$) or cNF ($p = 0.149$). In panel B, cNF significantly outperforms oversampling under unbiased sampling ($p < 0.001$), while the difference under biased sampling is not significant ($p = 0.072$); biased and unbiased sampling differ significantly for cNF ($p = 0.030$), indicating that urban-biased sampling can distort socioeconomic targets in ways that contextual conditioning does not fully absorb.

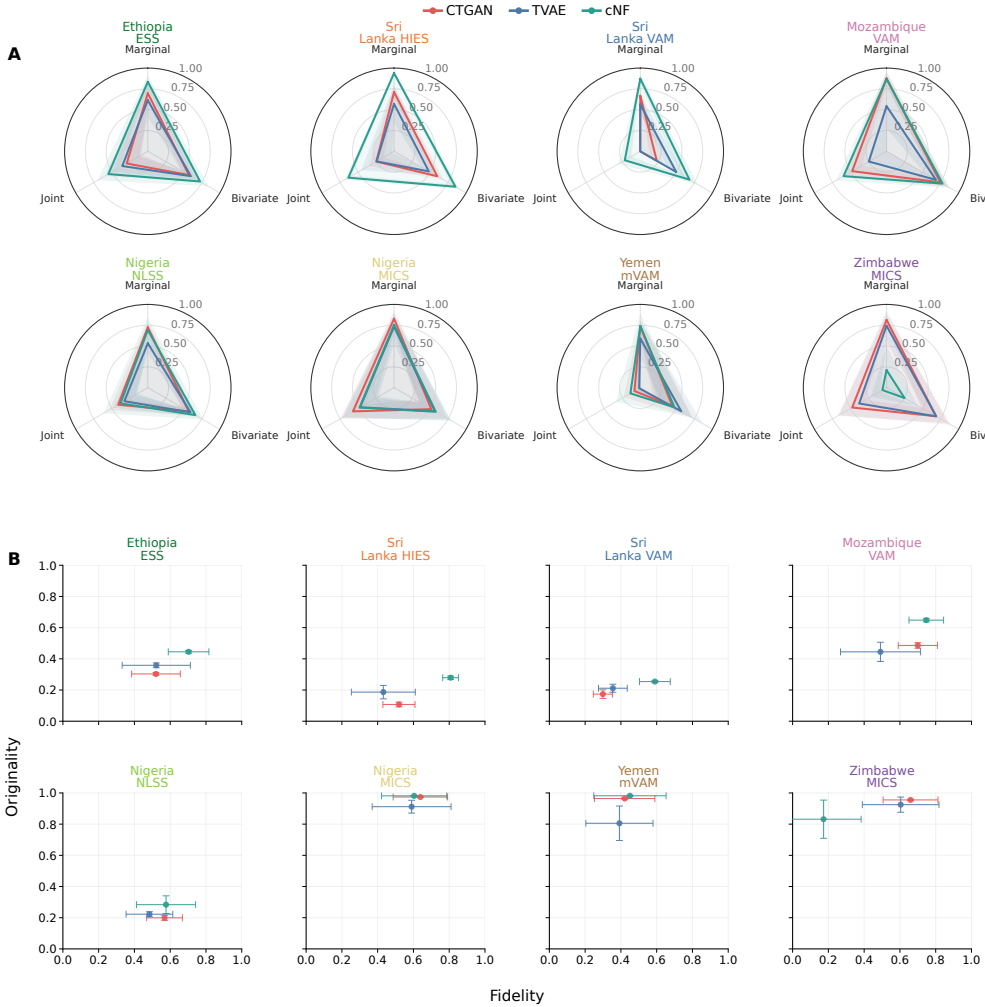


Figure S4: Synthetic data quality across generative models and survey experiments. (A) Radar plots showing fidelity of synthetic data generated by CTGAN, TVAE, and cNF across eight survey experiments. Each axis represents a distributional similarity metric (marginal, bivariate, and joint), expressed as $1 - \text{metric}$, where higher values indicate greater fidelity. Shaded regions indicate standard deviation across administrative units. **(B)** Fidelity–originality trade-off for each experiment. The x -axis shows average fidelity (mean of the three radar metrics), and the y -axis shows originality, measured as the recall of the real data distribution in the synthetic data. Error bars represent standard deviation across seeds. Points closer to the top-right corner indicate models that are simultaneously faithful to the real distribution and generative of sufficiently diverse synthetic samples.

Table S1: Dataset summary. For each dataset, the table reports the target variables, contextual information used, number of observations, number of administrative units at first-level administrative resolution, and summary statistics. Contextual information is abbreviated as follows: W = wealth proxy, M = market accessibility, and E = environment indicators.

| Country | Dataset | Variable | Context | N_full | first-level administrative unit | Min | Median | Max | | | | | |
|------------|----------|------------------------------------|---------|--------|---------------------------------|----------|-----------------|---------|-------|----|-----|------|-------|
| Ethiopia | Eth ESS | Education | W, M, E | 6214 | 11 | 0.0 | 3.5 | 35.0 | | | | | |
| | | Iron (mg) | | | | 0.0 | 26.6 | 370.2 | | | | | |
| | | Folate (μg) | | | | 0.0 | 216.6 | 3722.1 | | | | | |
| | | Expenditures | | | | 0.0 | 5.5 | 11.0 | | | | | |
| | | Vitamin A (μg RAE) | | | | 0.0 | 189.4 | 7250.9 | | | | | |
| | | Vitamin B_{12} (μg) | | | | 0.0 | 0.2 | 12.7 | | | | | |
| | | Zinc (mg) | | | | 0.0 | 13.0 | 110.4 | | | | | |
| Sri Lanka | Lka HIES | Education | W, M, E | 19911 | 9 | 0.0 | 10.0 | 19.5 | | | | | |
| | | Iron (mg) | | | | 0.0 | 12.8 | 56.0 | | | | | |
| | | Folate (μg) | | | | 0.0 | 202.3 | 756.1 | | | | | |
| | | Expenditures | | | | 5.7 | 12.1 | 18.4 | | | | | |
| | | Vitamin A (μg RAE) | | | | 0.0 | 199.2 | 1324.6 | | | | | |
| | | Vitamin B_{12} (μg) | | | | 0.0 | 1.1 | 11.1 | | | | | |
| | | Zinc (mg) | | | | 0.0 | 9.0 | 28.9 | | | | | |
| | Lka VAM | FCS | W, M, E | 14488 | 9 | 12.5 | 49.0 | 112.0 | | | | | |
| | | FES | | | | 0.0 | 0.6 | 1.0 | | | | | |
| | | Education | | | | 0.0 | 0.6 | 1.0 | | | | | |
| | | Income | | | | 9.2 | 11.4 | 14.9 | | | | | |
| | | rCSI | | | | 0.0 | 2.0 | 56.0 | | | | | |
| | | Space pp | | | | 0.0 | 0.8 | 6.0 | | | | | |
| Mozambique | Moz VAM | FCS | W, M, E | 11080 | 11 | 0.0 | 39.0 | 112.0 | | | | | |
| | | Protein | | | | 0.0 | 4.0 | 42.0 | | | | | |
| | | Vitamin A | | | | 0.0 | 5.0 | 42.0 | | | | | |
| | | rCSI | | | | 0.0 | 3.0 | 56.0 | | | | | |
| Nigeria | Nga NLSS | Education | W, M, E | 22106 | 37 | 0.0 | 9.0 | 20.0 | | | | | |
| | | Iron (mg) | | | | 0.0 | 13.1 | 94.0 | | | | | |
| | | Folate (μg) | | | | 0.0 | 229.2 | 1586.9 | | | | | |
| | | Expenditures | | | | 0.0 | 8.8 | 14.8 | | | | | |
| | | Vitamin A (μg RAE) | | | | 0.0 | 232.4 | 2982.9 | | | | | |
| | | Vitamin B_{12} (μg) | | | | 0.0 | 2.1 | 31.2 | | | | | |
| | | Zinc (mg) | | | | 0.0 | 6.9 | 101.3 | | | | | |
| | Nga MICS | Education | W, M, E | 39572 | 37 | 0.0 | 0.5 | 1.0 | | | | | |
| | | Space pp | | | | 0.1 | 0.4 | 74.0 | | | | | |
| | | Wealth score | | | | -2.8 | -0.2 | 2.9 | | | | | |
| | | Yemen | | | | Yem mVAM | FCS | W, M, E | 54702 | 22 | 0.5 | 34.0 | 112.0 |
| | | | | | | | Expenditures pp | | | | 2.1 | 9.1 | 15.9 |
| | | | | | | | rCSI | | | | 0.0 | 14.0 | 56.0 |
| Zimbabwe | Zwe MICS | Education | W, M, E | 11043 | 10 | 0.0 | 0.5 | 1.0 | | | | | |
| | | Space pp | | | | 0.1 | 0.5 | 5.0 | | | | | |
| | | Wealth score | | | | -1.3 | -0.5 | 3.2 | | | | | |